

Planar Tunneling and Andreev Reflection: Powerful probes of the superconducting order parameter

Laura H. Greene



Department of Physics
Center for Emergent Superconductivity
Frederick Seitz Materials Research Laboratory
Center for Nanoscale Science and Technology
University of Illinois at Urbana-Champaign
Urbana, IL 61801 USA
Ihgreene@illinois.edu

ICMR Summer School on Novel Superconductors

August 2 – 15, 2009

UCSB

Outline:

Lecture 1 (Tunneling spectroscopy on HTS):

- **Promo:** Grand statement / DoE-BES report / new SCs
- **Broken symmetries** (gauge, reflection and time-reversal)
- **Tunneling** and order parameter (OP) symmetry
- **Andreev reflection** (AR)
- **Tunneling** into Andreev bound states: Broken symmetries

Lecture 2 (Andreev reflection spectroscopy on HFs):

- Point Contact Andreev Reflection Spectroscopy (PCARS)
- Blonder-Tinkham-Klapwijk (BTK) theory and it's ext. to d-wave
- Definition of the issues (AR at HFSs and spectroscopy of HFs)
- CeCoIn5 and related HFs
- Describe data with a
 - two-fluid model and
 - Fano resonance in an energy-dependent DoS

Collaborators

Wan Kyu Park

(Illinois)

Xin Lu (Illinois)

Eric Bauer (LANL)

John L. Sarrao (LANL)

Joe D. Thompson (LANL)

Zack Fisk (UC Irvine)

Acknowledgements:

Phil Anderson, Donald Ginsberg*, Tony Leggett,
V. Lukic, David Pines, Heiko Stalzer,
Dozens of undergraduates, NSF, and DoE.

**in memory*

Group Seminar, Monday September 15, 2008

Introduction to Blonder-Tinkham-Klapwijk Theory and Point-Contact Spectroscopy

Wan Kyu Park

Outline

- Tunneling and Andreev reflection
- Blonder-Tinkham-Klapwijk theory
- Point-contact Spectroscopy
- Examples: Nb and MgB₂
- PCS of heavy fermions: CeCoIn5 and related)
- PCS of graphite

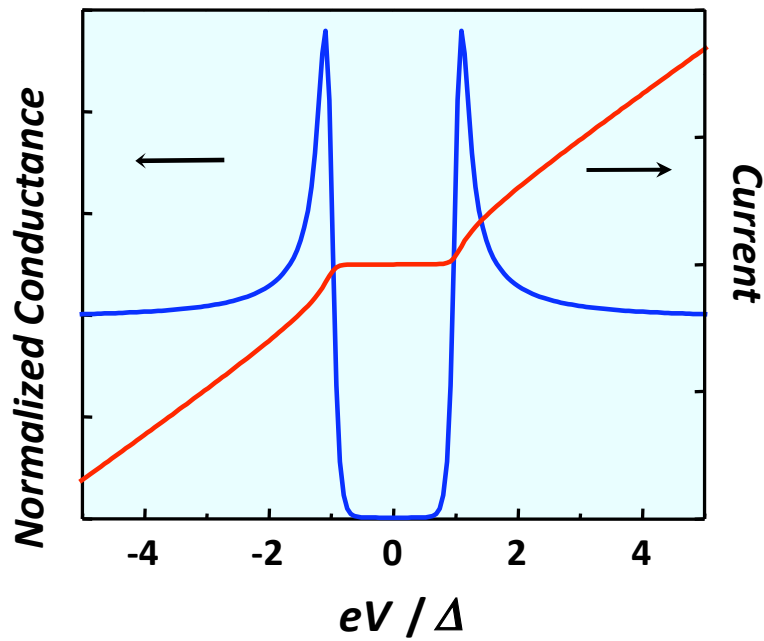
Electron Tunneling Spectroscopy (last lecture)

Tunnel Current: $I(V) = A|T|^2 e N_n(0) \int_{-\infty}^{\infty} N_s(E) [f(E - eV) - f(E)] dE$

Tunnel Conductance: $G(V) \equiv \frac{dI}{dV} = A|T|^2 e^2 N_n(0) \int_{-\infty}^{\infty} N_s(E) \frac{\partial f(E - eV)}{\partial(eV)} dE$

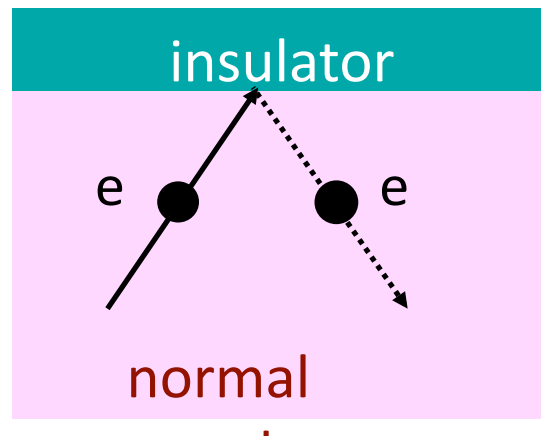
For $T = 0$, $\frac{\partial f(E - eV)}{\partial(eV)} = \delta(E - eV) \Rightarrow G(V) \propto N_s(eV).$

For $T > 0$, $G(V)$ is given as a Convolution of SC DOS w.r.t. Derivative of Fermi Function.



- Bias dependence of tunneling conductance directly probes DOS. \Rightarrow well established to probe SC gap.
- E. L. Wolf, *Electron tunneling spectroscopy*

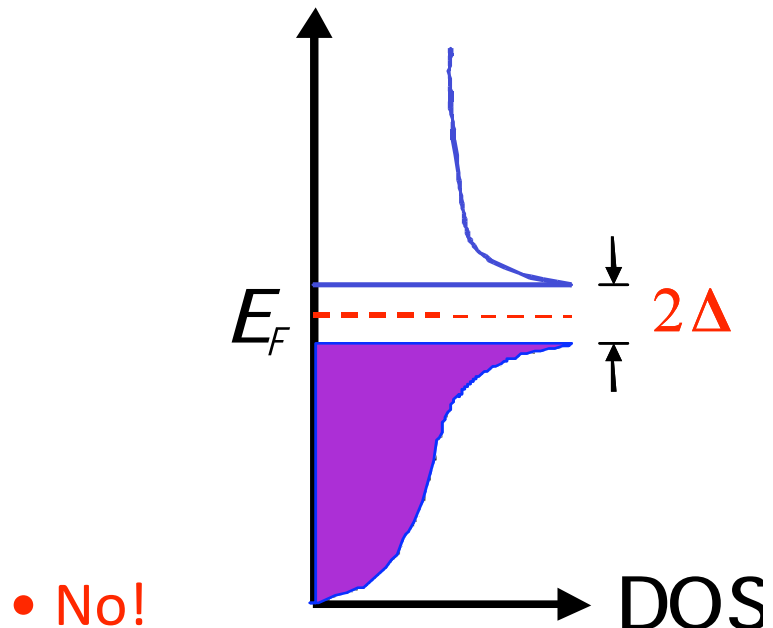
What will happen to an electron with $E < \Delta$ if \exists no tunnel barrier?



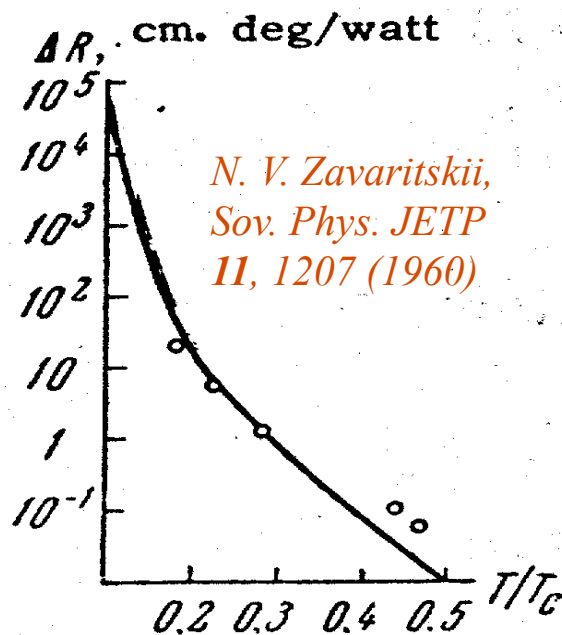
metal
specular reflection

- No QP states available, no single particles are allowed to enter S.
- Will a NS system be less conductive than a single S?

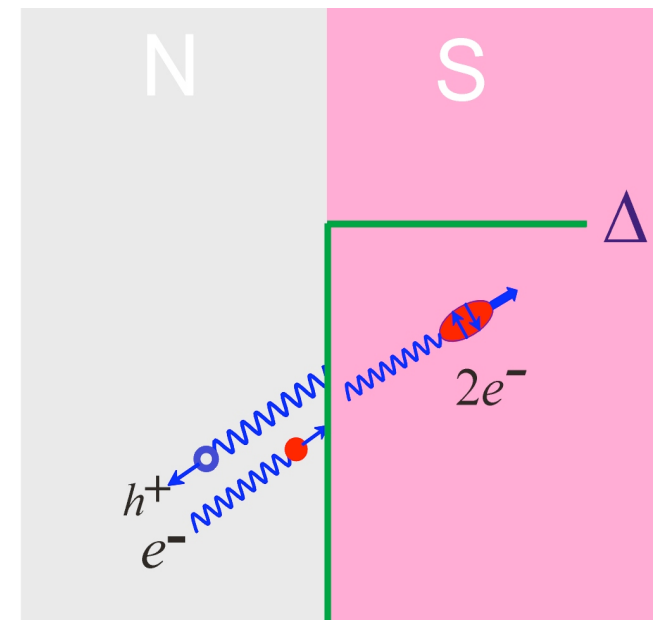
cf. At an interface with huge potential barrier that is translationally invariant along the transverse direction, incoming electrons reflect specularly.



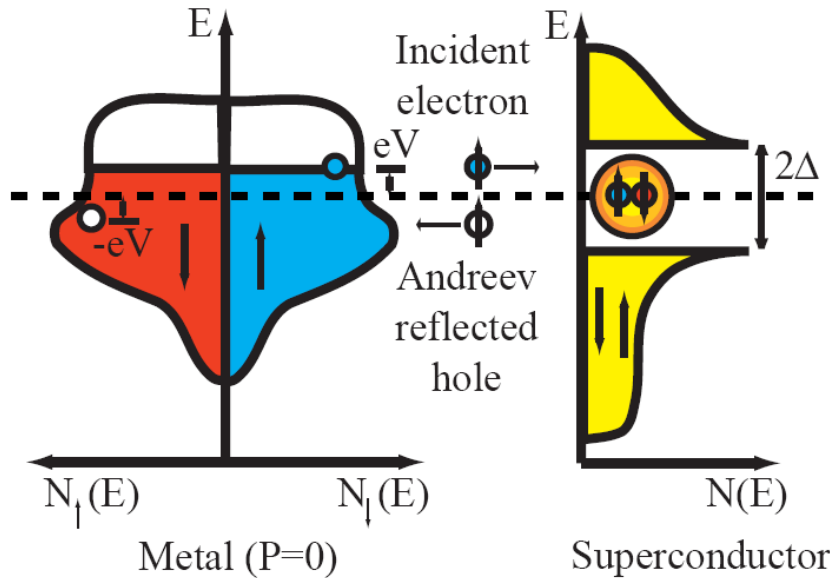
Andreev Reflection (I)



- QM scattering off SC pair potential near N/S
- Particle-hole conversion process multi-particle (AR) vs. single particle (tunneling)
- Retro-reflection $\mathbf{v}_h = -\mathbf{v}_e$

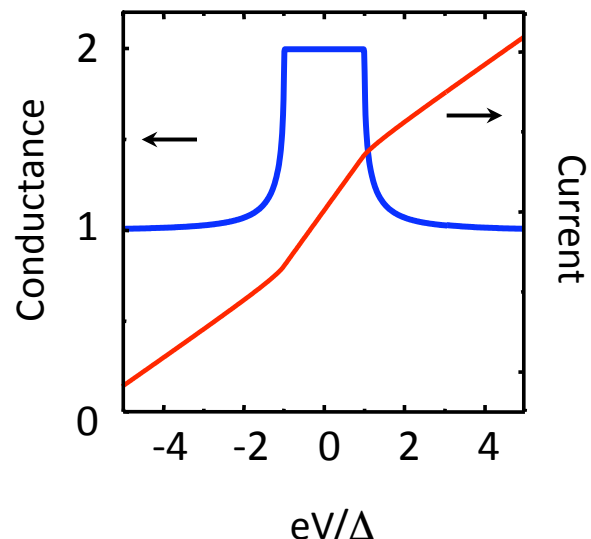


Andreev Reflection (II)



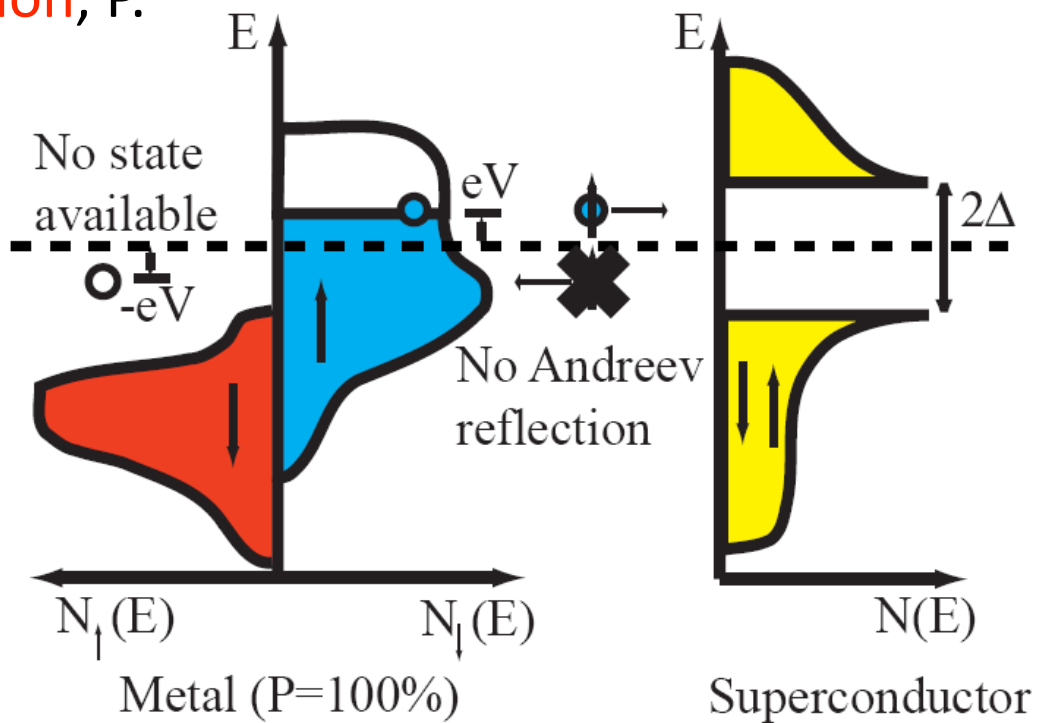
- Conserved quantities
 - Energy (E)
 - Momentum ($\hbar k$) ($\Delta \ll E_F$)
 - Spin (S)
 - Charge inc. Cooper pairs

- Sub-gap conductance is doubled.
- Andreev reflected hole carries information on the phase of electron state and macroscopic phase of SC. phase change = $\Phi + \arccos(\epsilon/\Delta)$
- Inverse process ($S \Rightarrow N$): AR of a hole or
 - emission of a Cooper pair ("Andreev pairs"): proximity effect



Andreev Reflection (III)

- If a metal electrode has unequal number of spin up and spin-down electrons as in ferromagnets or half metals, Andreev reflection is suppressed.
- Measuring conductance of FM/S junction gives information on **spin polarization**, P.

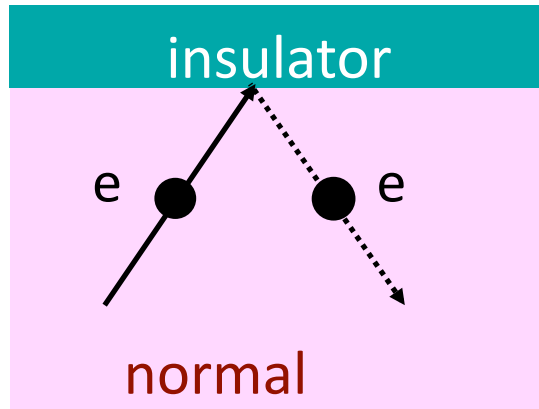


Andreev Reflection (IV)

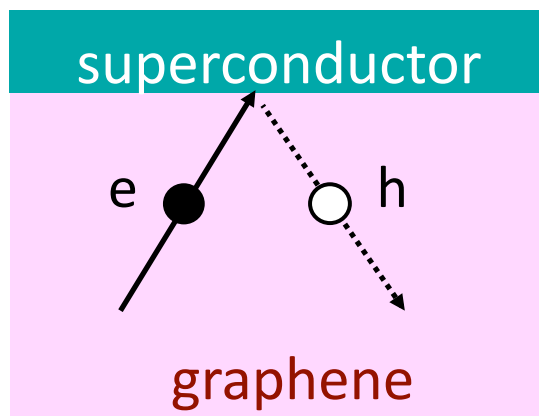
- Proximity effects: S/N, S/N/S (Josephson junction)
- Subharmonic gap structure: S/N/S (MAR, KBT & Octavio 1982-3)
- Reentrant behavior: mesoscopic S/N (vs. conjugated mirror)
- **Reflectionless tunneling**: S/I/DN (enhanced AR prob, ZBCP.)
- **Andreev bound states**: nodal surfaces of p - and d -wave SC
- Andreev interferometer
- Andreev billiard
- Crossed (or nonlocal) AR
- Kondo QD coupled to SC: interplay between AR & Kondo effect

Andreev reflection is an interesting and fascinating phenomenon, having various applications to superconducting devices, AND NORMAL STATE PROPERTIES !

Various Quasiparticle Reflections at Interfaces

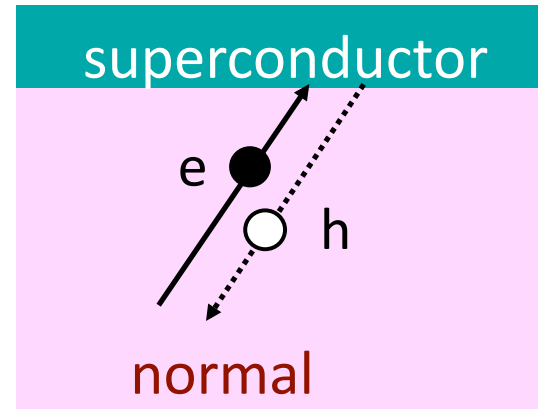


normal
specular reflection

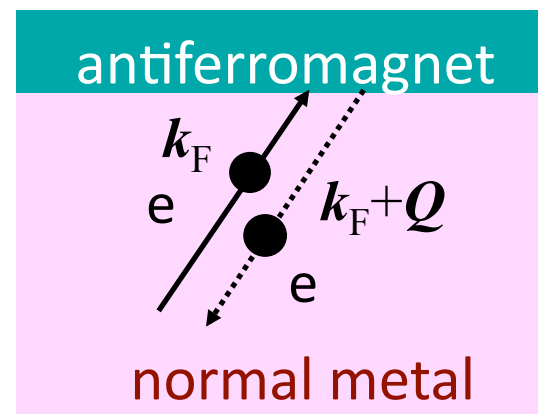


specular Andreev reflection

Beenakker, PRL (2006)



normal
Andreev retro-reflection



spin-dependent Q-reflection

Bobkova et al., PRL (2005)

Elementary QP Excitations in a SC

$$i\hbar \frac{\partial f}{\partial t} = \left[-\frac{\hbar^2}{2m} \nabla^2 - \mu(x) + V(x) \right] f(x, t) + \Delta(x) g(x, t)$$

$$i\hbar \frac{\partial g}{\partial t} = - \left[-\frac{\hbar^2}{2m} \nabla^2 - \mu(x) + V(x) \right] g(x, t) + \Delta(x) f(x, t)$$

Bogoliubov – de
Gennes (BdG)
Equations

Assume $\mu(x) = \mu$, $V(x) = 0$, $\Delta(x) = \Delta$.

Plane wave solutions

$$f = \tilde{u} e^{ikx - iEt/\hbar}$$

$$g = \tilde{v} e^{ikx - iEt/\hbar}$$



$$\begin{bmatrix} \left(\frac{\hbar^2 k^2}{2m} - \mu \right) & \Delta \\ \Delta & - \left(\frac{\hbar^2 k^2}{2m} - \mu \right) \end{bmatrix} \begin{bmatrix} \tilde{u} \\ \tilde{v} \end{bmatrix} = E \begin{bmatrix} \tilde{u} \\ \tilde{v} \end{bmatrix}$$

BCS Quasiparticle: Bogoliubon

Solving for E, \tilde{u}, \tilde{v} ,

$$E^2 = \left(\frac{\hbar^2 k^2}{2m} - \mu \right)^2 + \Delta^2$$

$$\hbar k^\pm = \sqrt{2m\mu} \sqrt{1 \pm \frac{\sqrt{E^2 - \Delta^2}}{\mu}}$$

$$\hbar q^\pm = \sqrt{2m} \sqrt{\mu \pm E} \text{ for N } (\Delta=0)$$

$$\tilde{u}^2 = \frac{1}{2} \left(1 \pm \frac{\sqrt{E^2 - \Delta^2}}{E} \right) = 1 - \tilde{v}^2$$

$$u_0^2 \equiv \frac{1}{2} \left(1 + \frac{\sqrt{E^2 - \Delta^2}}{E} \right) = 1 - v_0^2$$

$$(u_0 > v_0)$$

Four types of QP waves for a given E

$$\text{Defining } \psi = \begin{pmatrix} f(x) \\ g(x) \end{pmatrix},$$

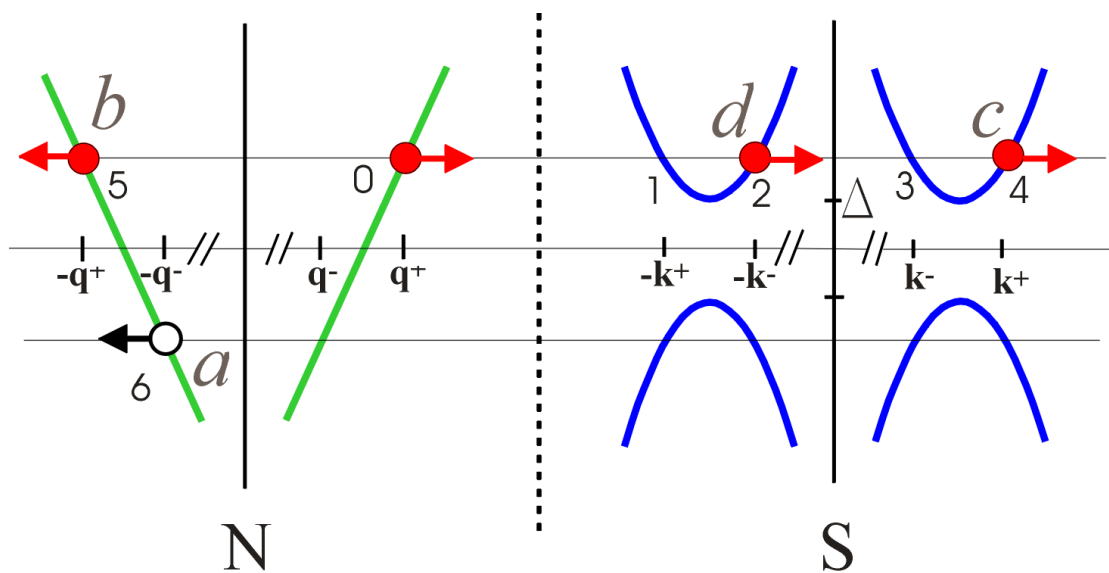
$$\psi_{\pm k^+} = \begin{pmatrix} u_0 \\ v_0 \end{pmatrix} e^{\pm i k^+ x}, \quad \psi_{\pm k^-} = \begin{pmatrix} v_0 \\ u_0 \end{pmatrix} e^{\pm i k^- x}$$

Bogoliubon: QP – a coherent combination of an electron-like and hole-like excitations

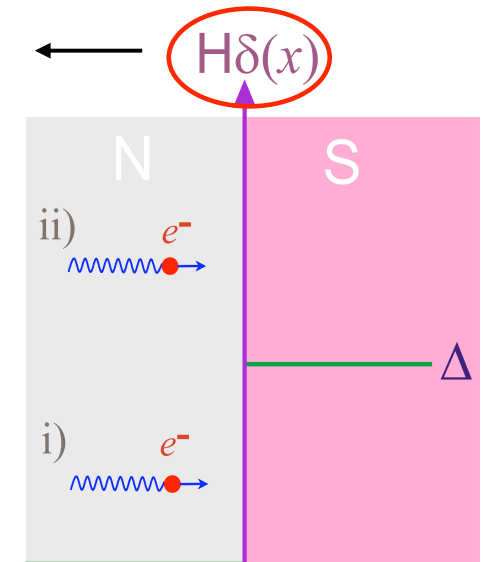
Blonder-Tinkham-Klapwijk Model

PRB 25, 4515 (1982), cf. Klapwijk for history, J. Supercond. 17, 593 (2004)

What is the fate of an electron approaching an N/S interface?



Potential barrier



Four trajectories are possible.

a : Andreev reflection

b : Normal reflection

c : Transmission without branch-crossing

d : Transmission with branch-crossing

Boundary Condition Problem

Boundary Conditions

i) $\psi_s(0) = \psi_n(0) \equiv \psi(0)$

ii) $\frac{\hbar}{2m} (\psi_s' - \psi_n') = H\psi(0)$

iii) wave directions are defined
by group velocities

$$\boxed{\begin{aligned} A &= aa^*, & a &= \frac{u_0 v_0}{\gamma} \\ B &= bb^*, & b &= -\frac{u_0^2 - v_0^2}{\gamma} (Z^2 + iZ) \\ C &= cc^*, & c &= \frac{u_0 (1 - iZ)}{\gamma} \\ D &= dd^*, & d &= \frac{iv_0 Z}{\gamma} \end{aligned}}$$

Trial Wave Functions

$$\psi_{inc} = \begin{pmatrix} 1 \\ 0 \end{pmatrix} e^{iq^+ x},$$

$$\psi_{refl} = a \begin{pmatrix} 0 \\ 1 \end{pmatrix} e^{iq^- x} + b \begin{pmatrix} 1 \\ 0 \end{pmatrix} e^{-iq^+ x},$$

$$\psi_{trans} = c \begin{pmatrix} u_0 \\ v_0 \end{pmatrix} e^{ik^+ x} + d \begin{pmatrix} v_0 \\ u_0 \end{pmatrix} e^{-ik^- x}$$

$$\gamma = u_0^2 + (u_0^2 - v_0^2) Z^2$$

$$u_0^2 = 1 - v_0^2 = \frac{1}{2} \left\{ + (E^2 - \Delta^2)^{1/2} / E \right\}$$

$$Z = \frac{mH}{\hbar^2 k_F} = H / \hbar v_F : \text{barrier strength}$$

$$Z_{eff} = \sqrt{Z^2 + \frac{(1-r)^2}{4r}}, \quad r \equiv \frac{v_{FN}}{v_{FS}}$$

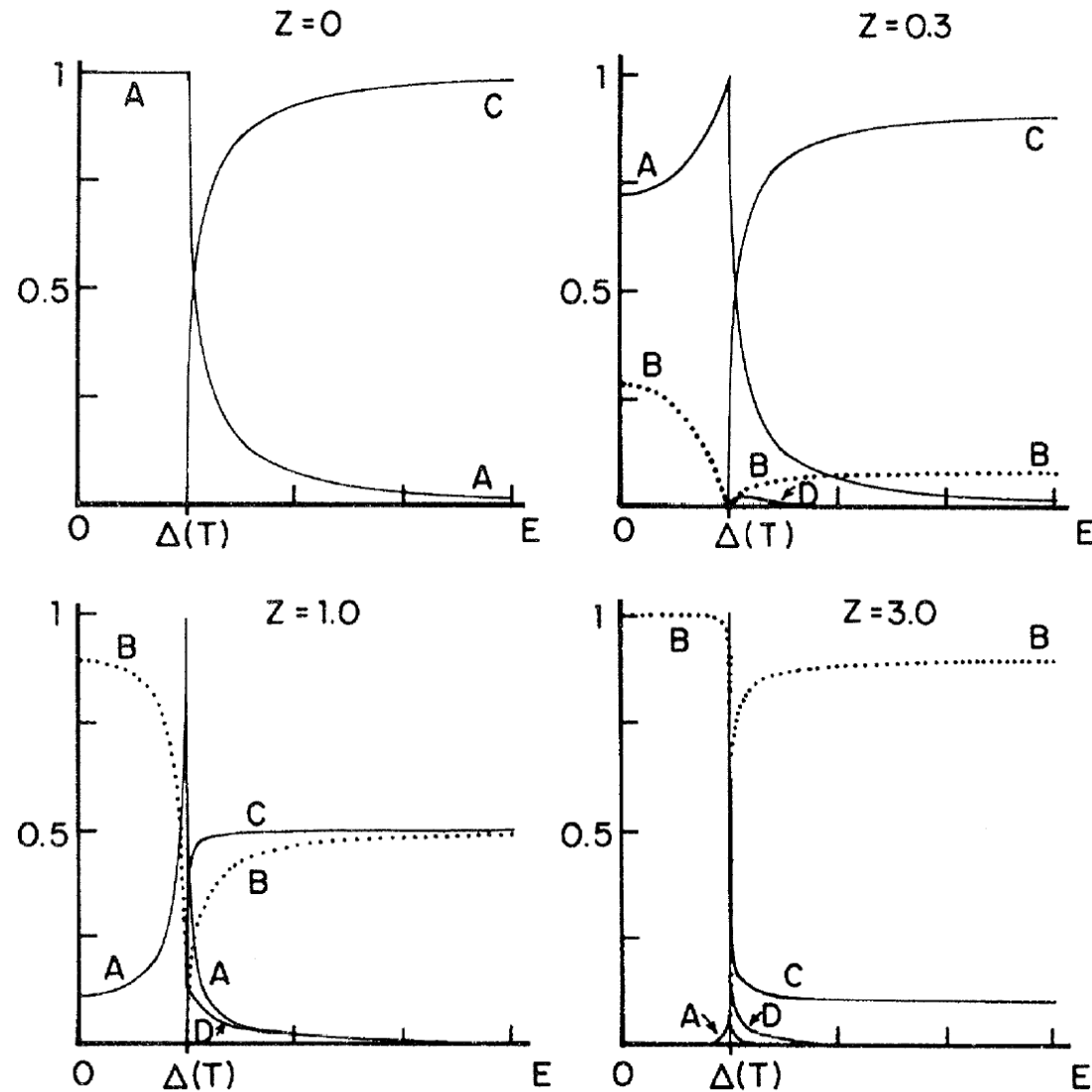
Reflection and Transmission Probabilities

	<i>A</i>	<i>B</i>	<i>C</i>	<i>D</i>
Normal state	0	$\frac{Z^2}{1+Z^2}$	$\frac{1}{1+Z^2}$	0
General form				
$E < \Delta$	$\frac{\Delta^2}{E^2 + (\Delta^2 - E^2)(1 + 2Z^2)^2}$	$1 - A$	0	0
$E > \Delta$	$\frac{u_0^2 v_0^2}{\gamma^2}$	$\frac{(u_0^2 - v_0^2)^2 Z^2 (1 + Z^2)}{\gamma^2}$	$\frac{u_0^2 (u_0^2 - v_0^2) (1 + Z^2)}{\gamma^2}$	$\frac{v_0^2 (u_0^2 - v_0^2) Z^2}{\gamma^2}$
No barrier ($Z = 0$)				
$E < \Delta$	1	0	0	0
$E > \Delta$	v_0^2 / u_0^2	0	$1 - A$	0
Strong barrier [$Z^2(u^2 - v^2) \gg 1$]				
$E < \Delta$	$\frac{\Delta^2}{4Z^2(\Delta^2 - E^2)}$	$1 - A$	0	0
$E > \Delta$	$\frac{u_0^2 v_0^2}{Z^4(u_0^2 - v_0^2)^2}$	$1 - \frac{1}{Z^2(u_0^2 - v_0^2)}$	$\frac{u_0^2}{Z^2(u_0^2 - v_0^2)}$	$\frac{v_0^2}{Z^2(u_0^2 - v_0^2)}$

$A = AR, B = NR, C = TM$ w/ branch crossing (BC), $D = TM$ w / BC

$$A+B+C+D=1$$

Probabilities (Cont'd)



- $A(E)$ peaks at Δ for $Z > 0$. \Rightarrow double peaks in dI/dV vs. V curve
- At $E = \Delta$, $A = 1$, $B = C = D = 0$, independent of Z .

I-V & dI/dV -V Formulas

$$I(V) = \int J$$

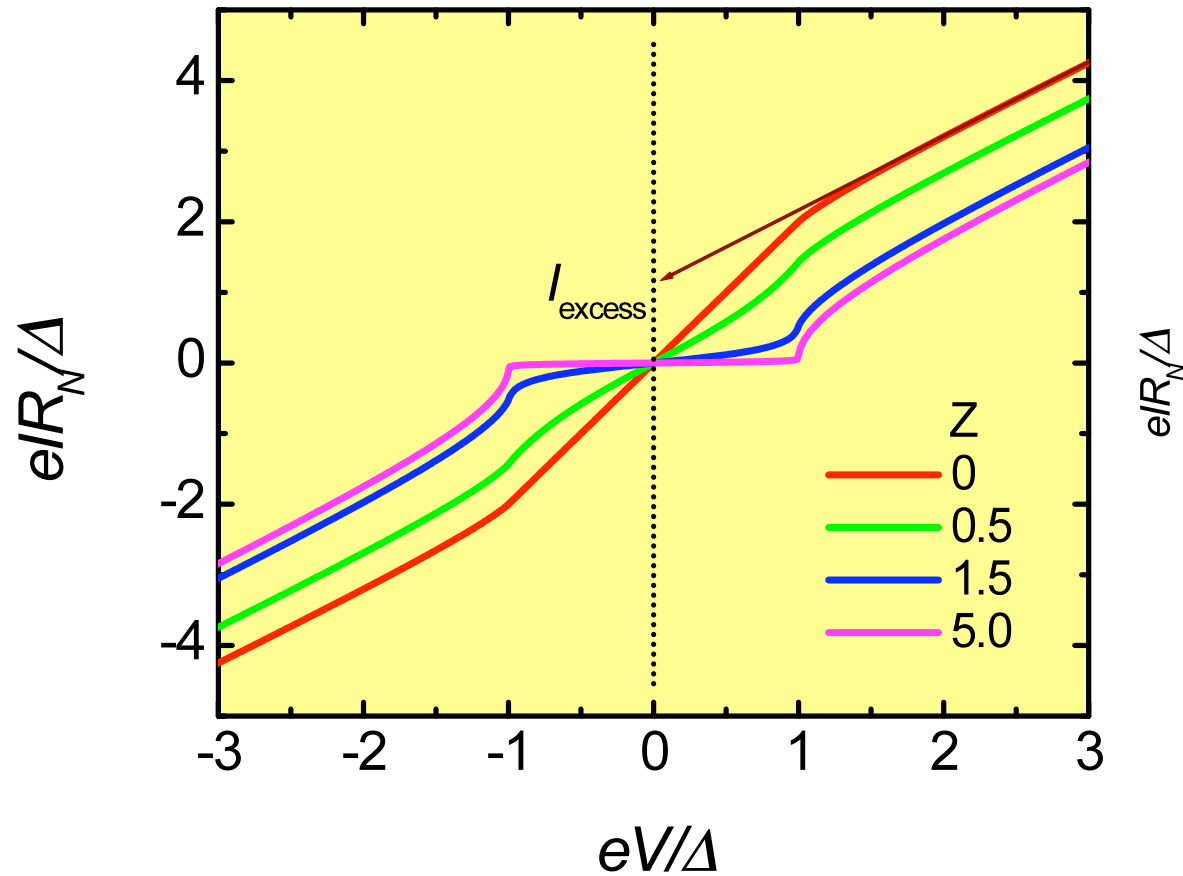
$$\begin{aligned} &= 2N(0)e\nu_F \int_{-\infty}^{\infty} dE [f_-(E) - f_+(E)] \\ &= 2N(0)e\nu_F \int_{-\infty}^{\infty} dE [f_0(E - eV) - f_0(E)] [1 + A(E) - B(E)] \\ &= 2N(0)e\nu_F \int_{-\infty}^{\infty} dE \left[\frac{1}{1 + \exp\left(\frac{E - eV}{kT}\right)} - \frac{1}{1 + \exp\left(\frac{E}{kT}\right)} \right] [1 + A(E) - B(E)] \end{aligned}$$

$$\begin{aligned} \frac{dI}{dV}(V) &= 2N(0)e\nu_F \int_{-\infty}^{\infty} \frac{\partial f_0(E - eV)}{\partial(eV)} [1 + A(E) - B(E)] dE \\ &= 2N(0)e^2\nu_F \int_{-\infty}^{\infty} dE \frac{\exp\left(\frac{E - eV}{kT}\right)}{kT \left[1 + \exp\left(\frac{E - eV}{kT}\right)\right]^2} [1 + A(E) - B(E)] \end{aligned}$$

How to Calculate BTK Conductance?

- Numerical integration using MATLAB®
- Original BTK kernel
 - singular points of the integrand
 - different formulas for $E < \Delta$ and $E > \Delta$.
- To fit exp. data, use three fitting parameters
 - Z: dimensionless barrier strength (0: metallic, ~ 5 : tunnel limit)
 - Δ : energy gap (peak position)
 - Γ : (Dynes) QP lifetime broadening factor, $\Gamma = h/2\pi\tau$
- How to incorporate Γ ?
 - replace $E \rightarrow E - i\Gamma$ in a , b , & calculate $A = aa^*$, $B = bb^*$
 - very complicated to do this!
- d-wave BTK Kernel developed by Tanaka & Kashiwaya gives the same results for s-wave SC but much more convenient to use.

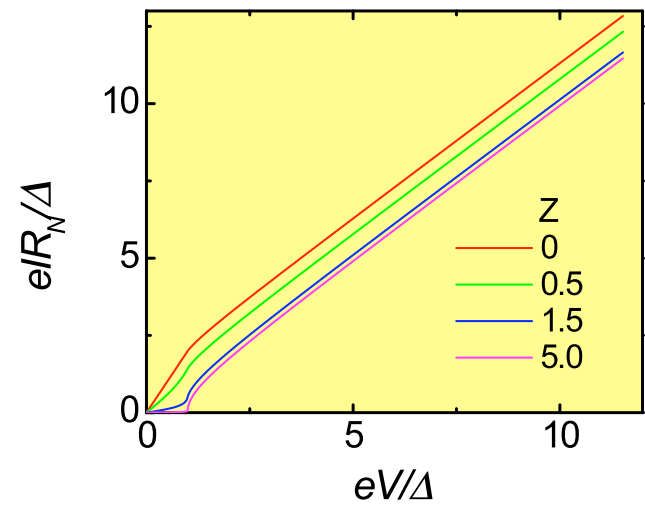
Current vs. Voltage Characteristics (Z-dep.)



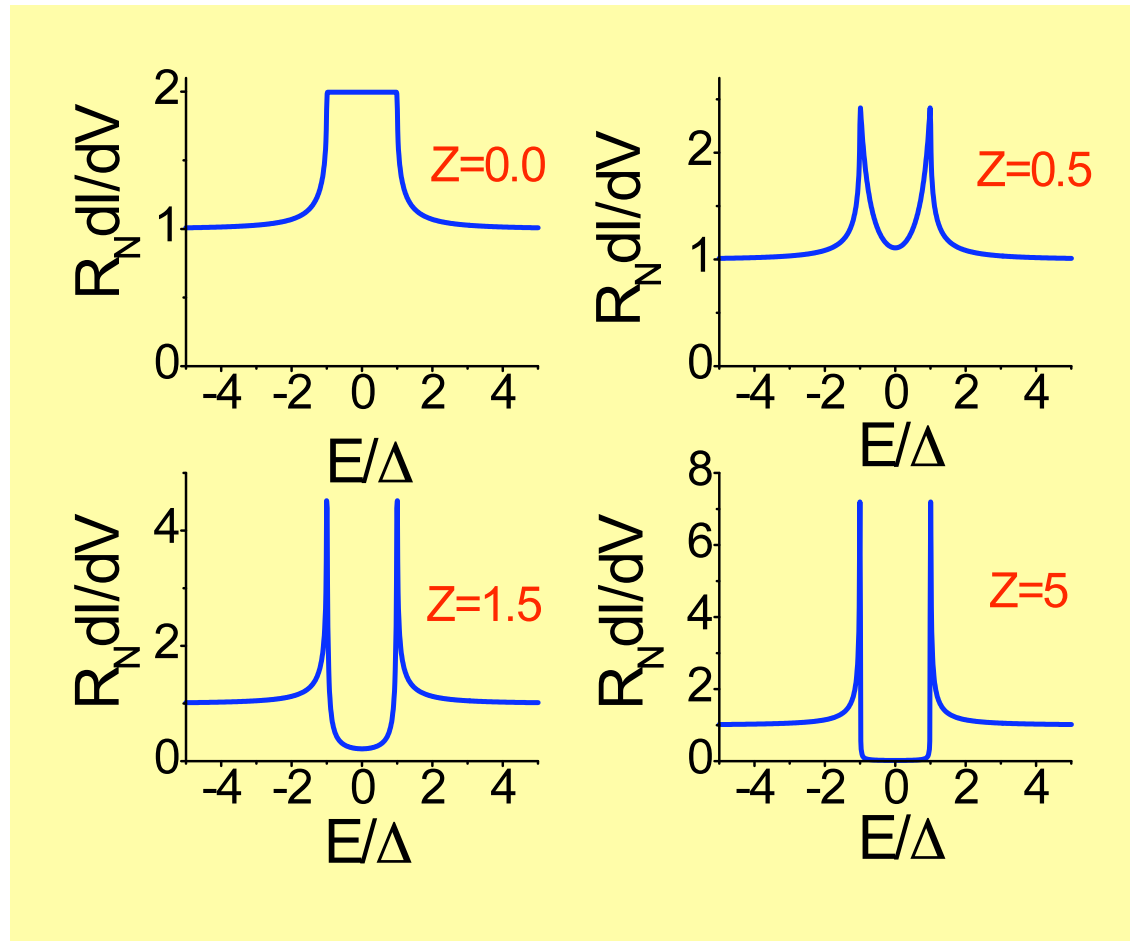
Excess current

$$I_{exc} \equiv (I_{NS} - I_{NN})|_{eV \gg \Delta}$$

$$I_{exc}(V) = (4\Delta/3eR_N) \tanh(eV/2kT), \quad \Delta \ll T$$



Conductance vs. Voltage Characteristics (Z-dep.)



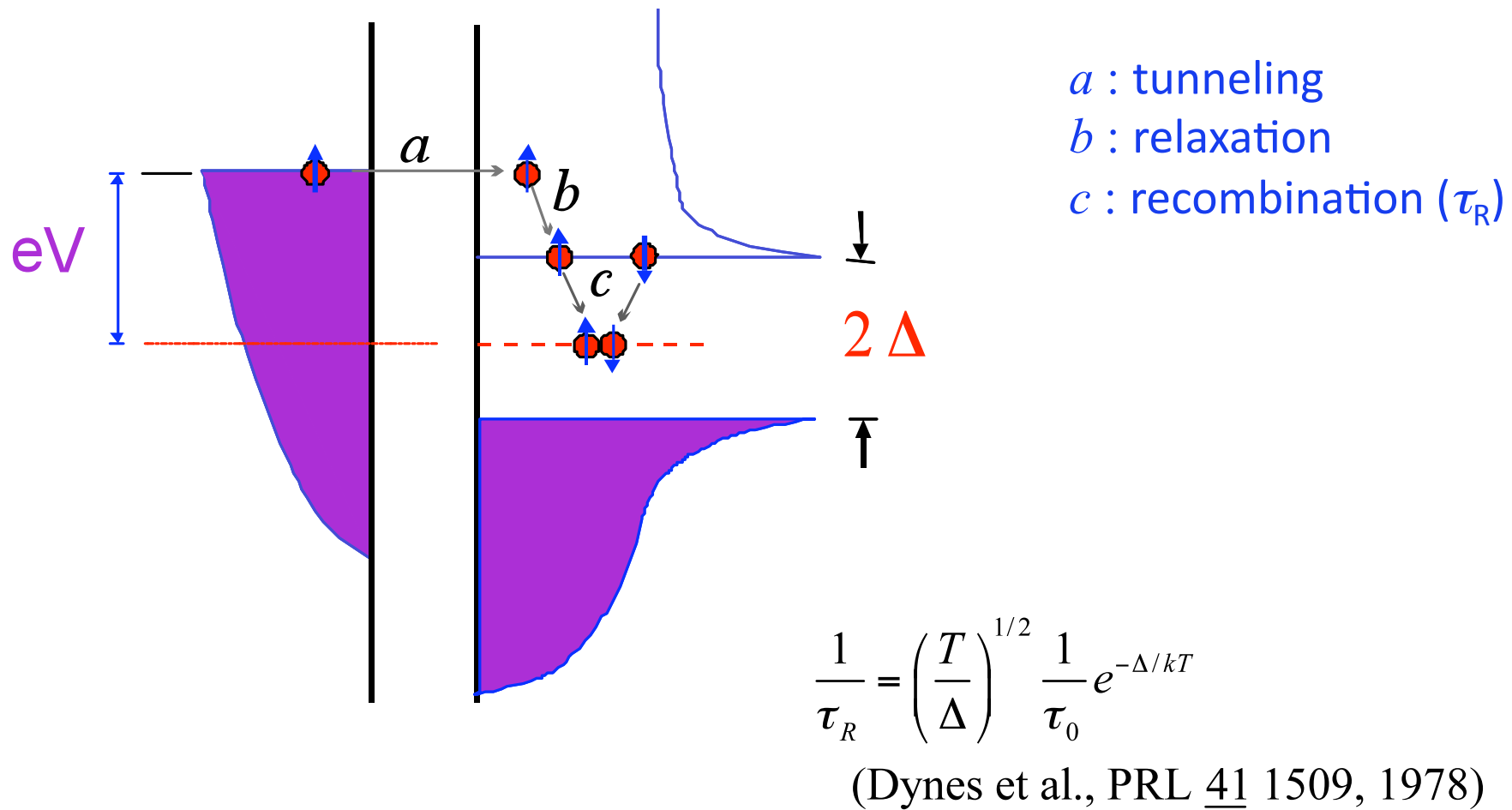
With increasing Z ,
AR →
Tunneling

$$Z = \sqrt{Z_0^2 + \frac{(1-r)^2}{4r}}, \quad r \equiv \frac{v_{FN}}{v_{FS}}$$

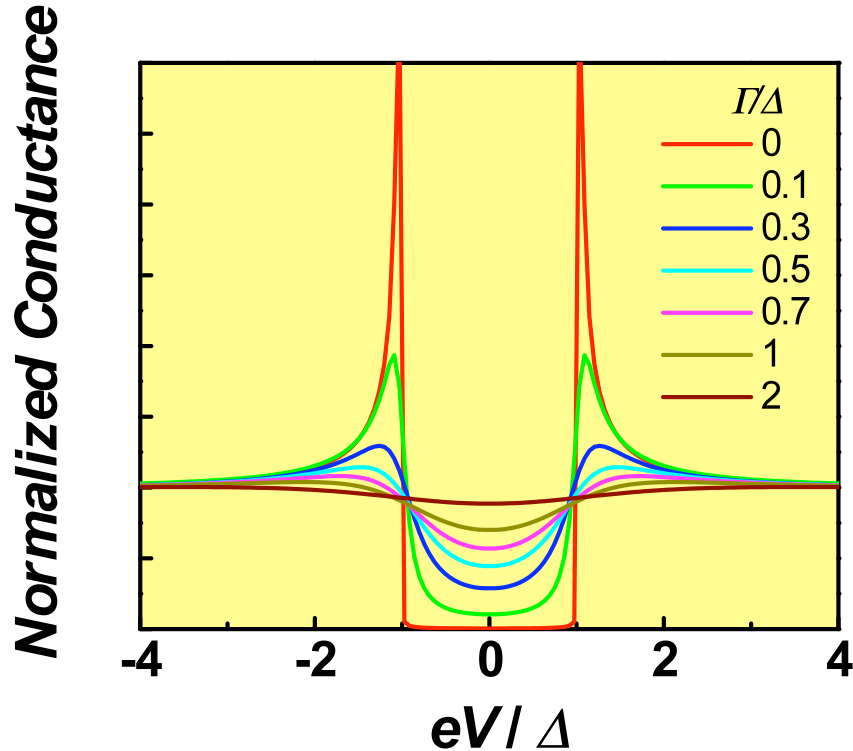
Is AR observable in heavy fermions?

Quasiparticle Lifetime

Consider, e.g., tunneling processes in a N/I/S junction.

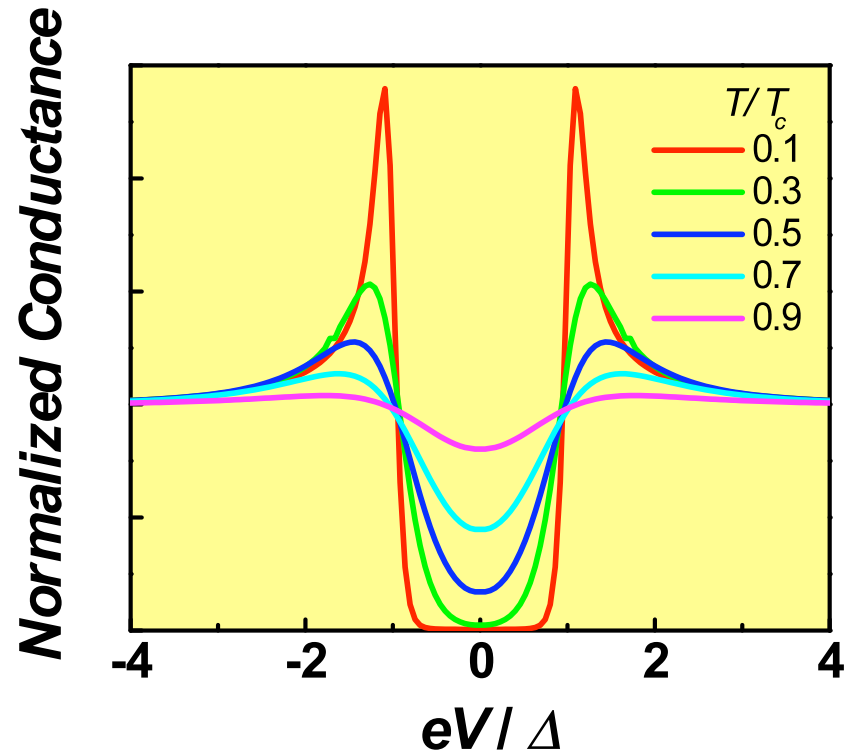


Quasiparticle vs. Thermal Smearing (Large Z)



$Z = 10, T = 0$

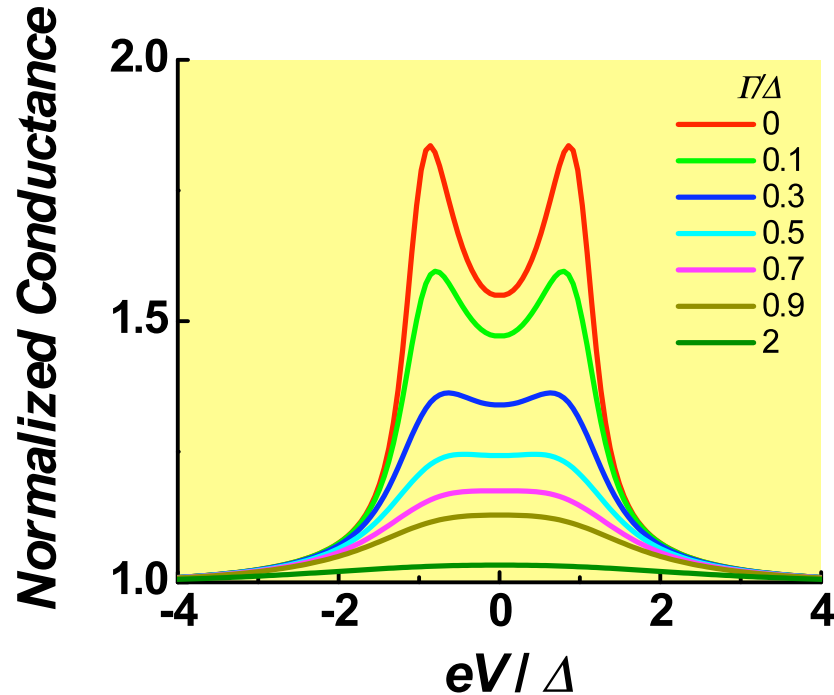
Smearing due to finite lifetime
of transferred QP



$Z = 10, \Gamma = 0$

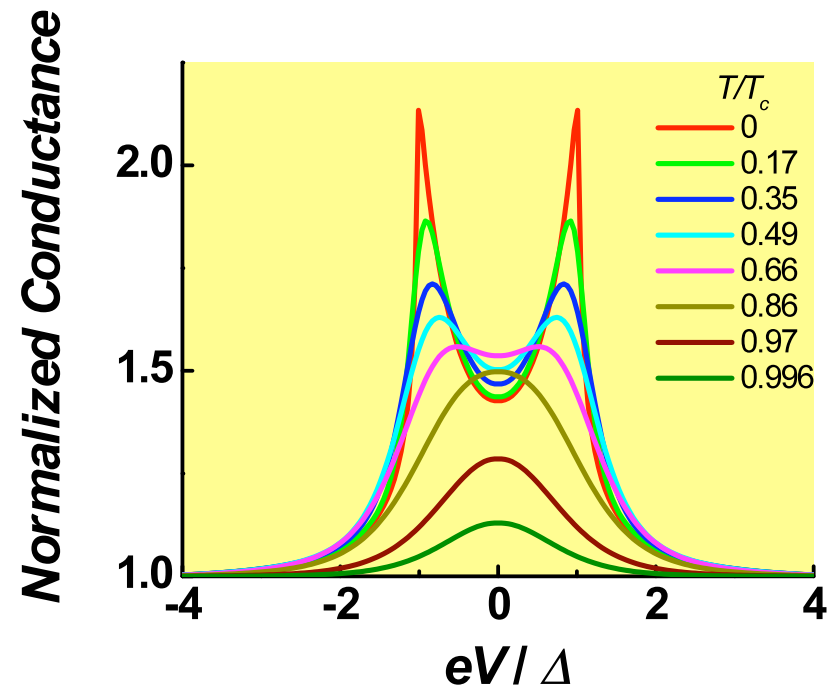
Smearing due to broadening
of Fermi function

Quasiparticle vs. Thermal Smearing (Small Z)



$Z = 0.308, T = 0$

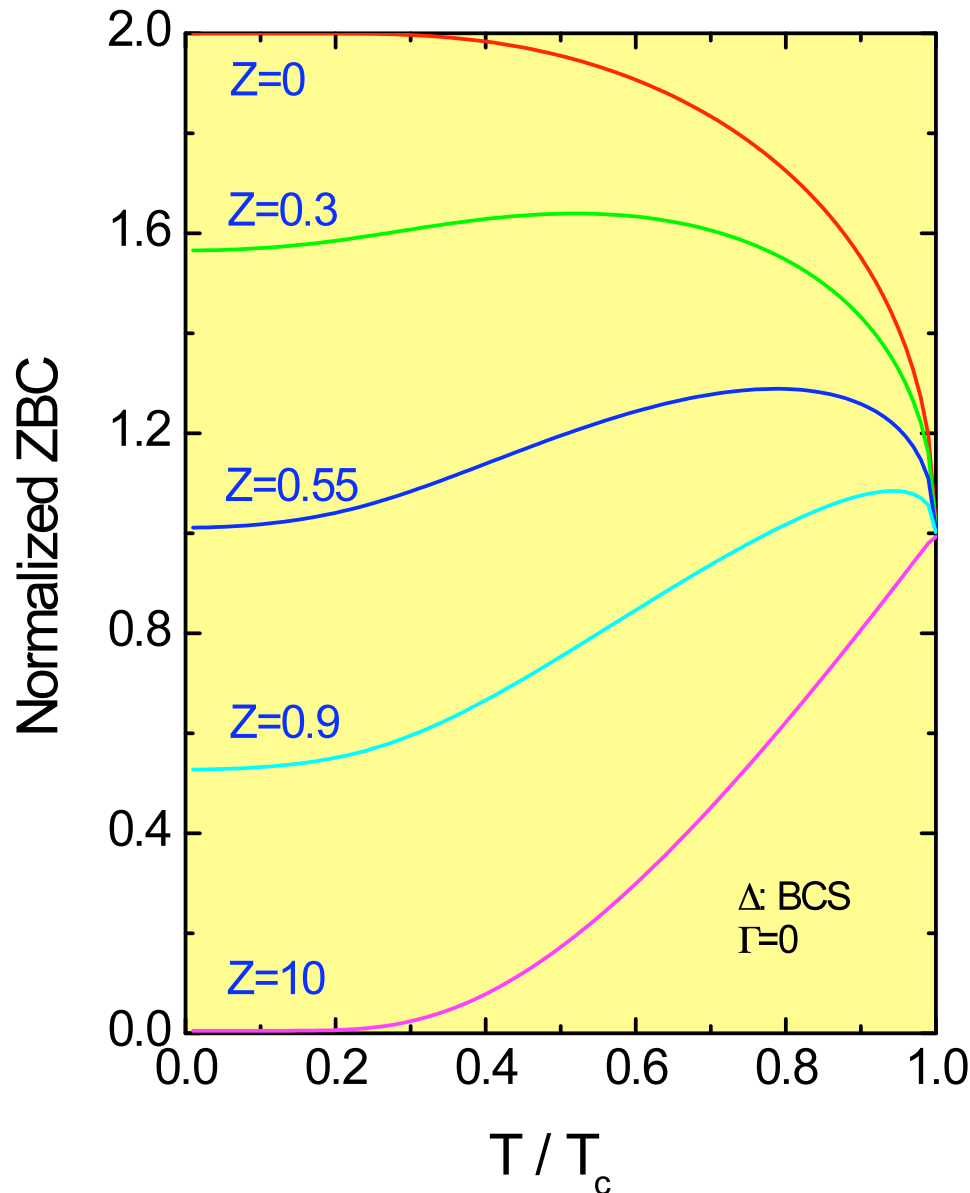
Smearing due to finite
“lifetime” of transferred QP



$Z = 0.35, \Gamma = 0$

Smearing due to broadening
of Fermi function

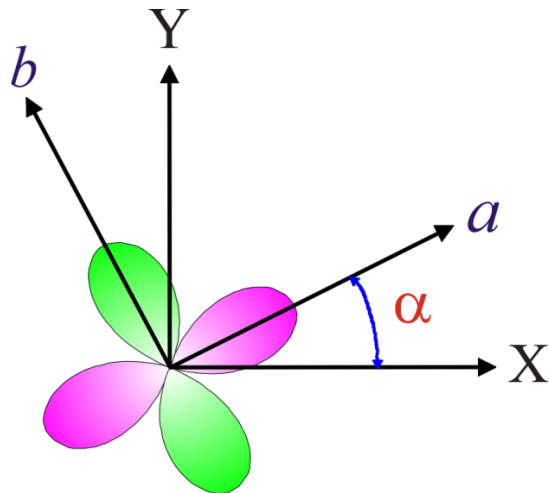
Zero-bias Conductance vs. Temperature (Z-dep.)



- ZBC vs. Temp. w/ inc. Z
- AR →
- Tunneling
- Useful to characterize the type of N/S junction
 - Could be used to estimate local T_c

Extended BTK theory (to d-wave)

S. Kashiwaya et al., PRB 53, 2667 (1996)



c-axis junction of d-wave superconductor

$$\Delta(T, \phi) = \Delta(T) \cos 2\phi$$

$$\Delta_+ = \Delta_-, \quad \varphi_+ = \varphi_-, \quad \Gamma_+ = \Gamma_- = \frac{E - \sqrt{E^2 - |\Delta|^2}}{|\Delta|}$$

The conductance is given by
the integration over the half space of momentum

$$\begin{aligned} \sigma_s(E) &= 1 + |a(E)|^2 - |b(E)|^2 \\ &= \sigma_N \frac{1 + \sigma_N |\Gamma_+|^2 + (\sigma_N - 1) |\Gamma_+ \Gamma_-|^2}{1 + (\sigma_N - 1) \Gamma_+ \Gamma_- \exp(i\varphi_- - i\varphi_+)^2} \end{aligned}$$

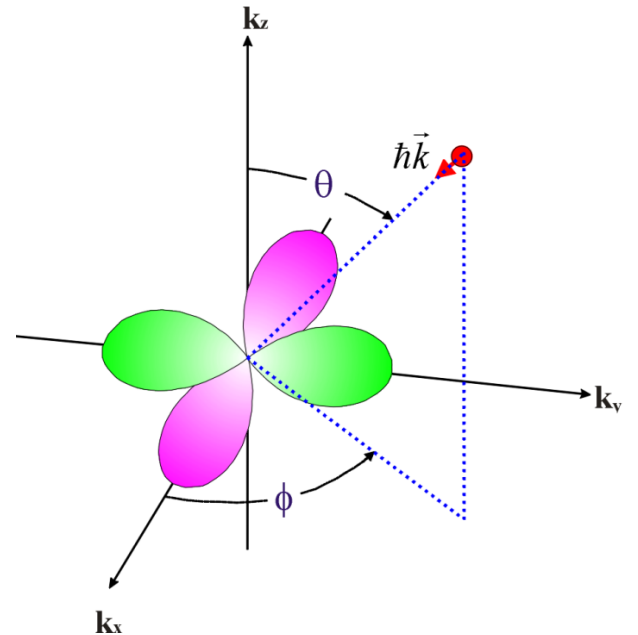
$$\Gamma_{\pm} = \frac{E - \Omega_{\pm}}{|\Delta_{\pm}|}, \quad \Omega_{\pm} = \sqrt{E^2 - |\Delta_{\pm}|^2}, \quad \Delta_{\pm} \equiv \Delta(\pm k_{FS}^{\pm}/k_{FN}) = |\Delta_{\pm}| \exp(i\varphi_{\pm})$$

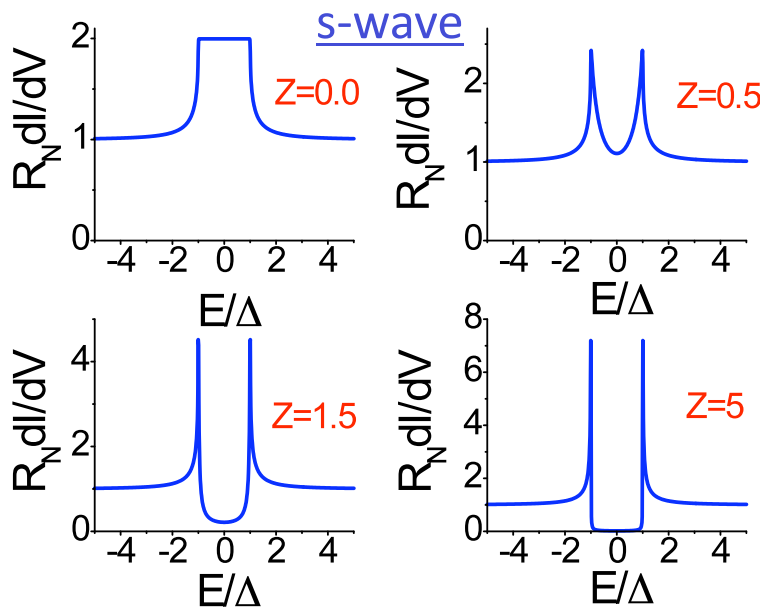
$$\lambda = \lambda_0 \frac{\cos \theta_S}{\cos \theta_N}, \quad \lambda_0 \equiv \frac{k_{FS}}{k_{FN}}, \quad k_{FS} \sin \theta_S = k_{FN} \sin \theta_N$$

$$Z = \frac{Z_0}{\cos \theta_N}, \quad Z_0 \equiv \frac{mH}{\hbar^2 k_{FN}}$$

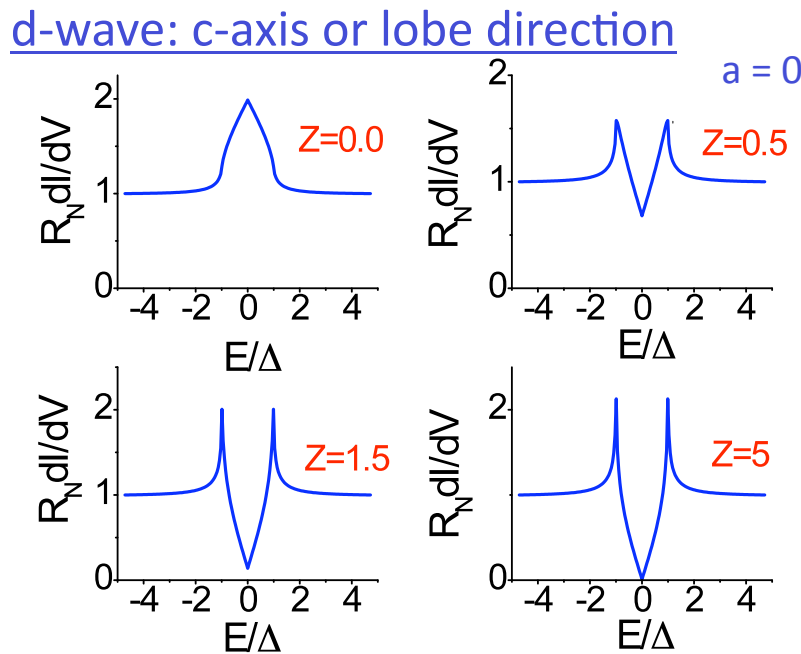
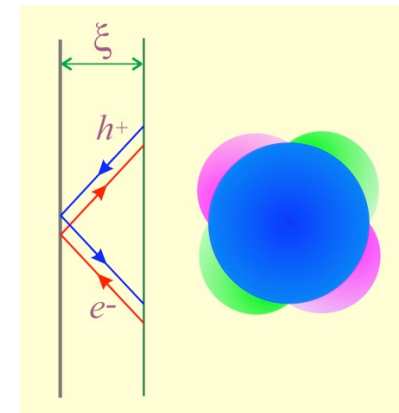
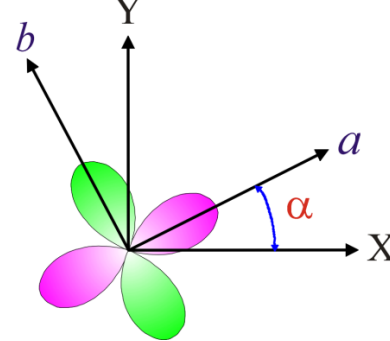
$$\sigma_N \equiv \frac{4\lambda}{(1+\lambda)^2 + 4Z^2}$$

$$E' = E - i\Gamma, \quad \Gamma = \frac{\hbar}{\tau}$$

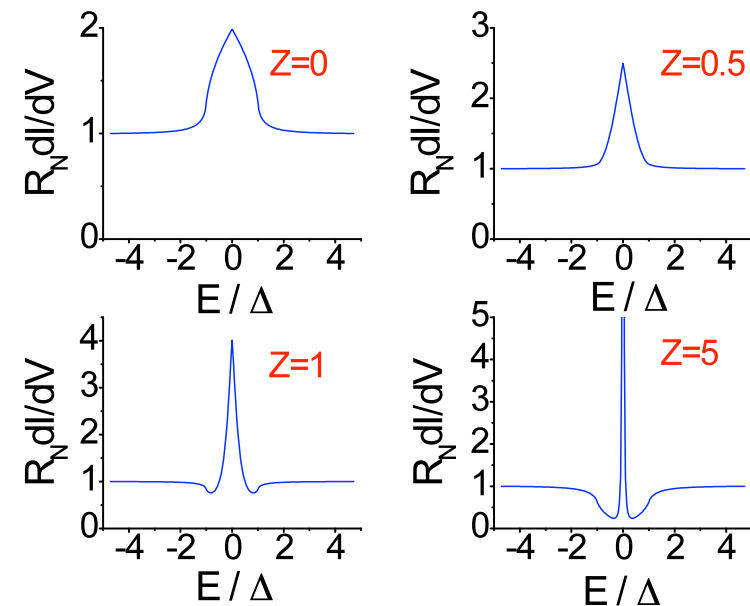




BTK Model for *s*-wave and extended to *d*-wave.

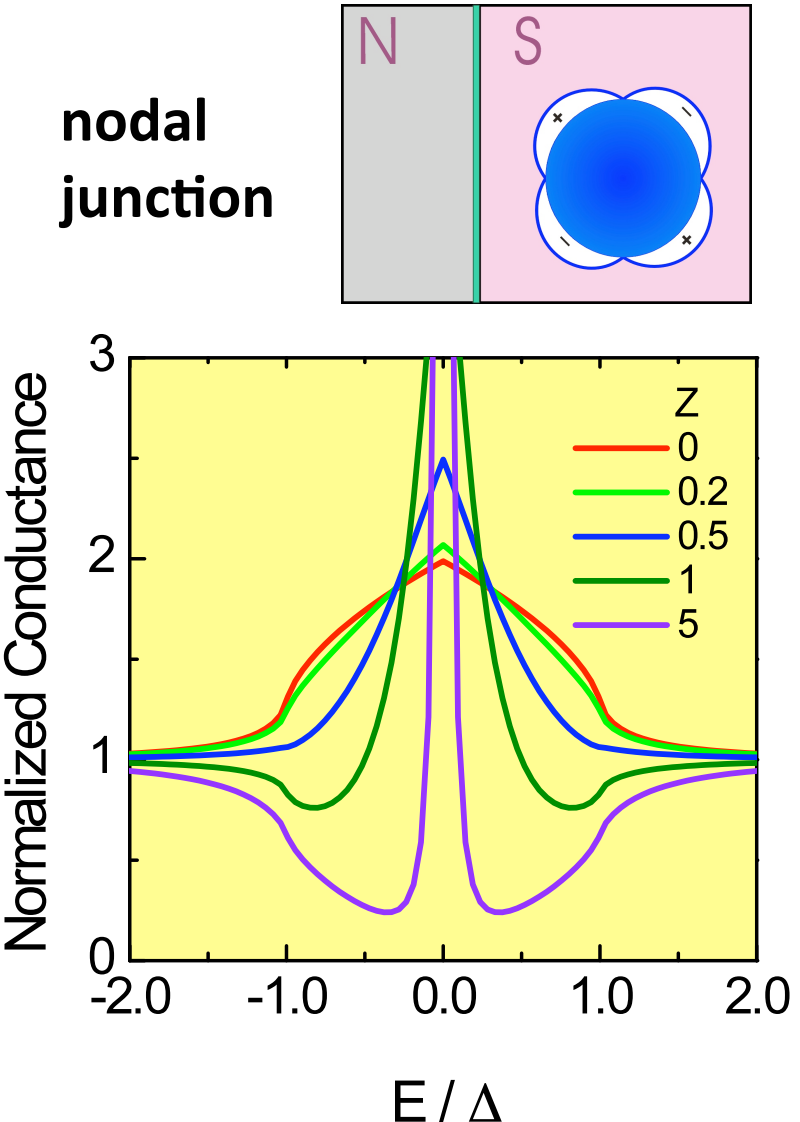
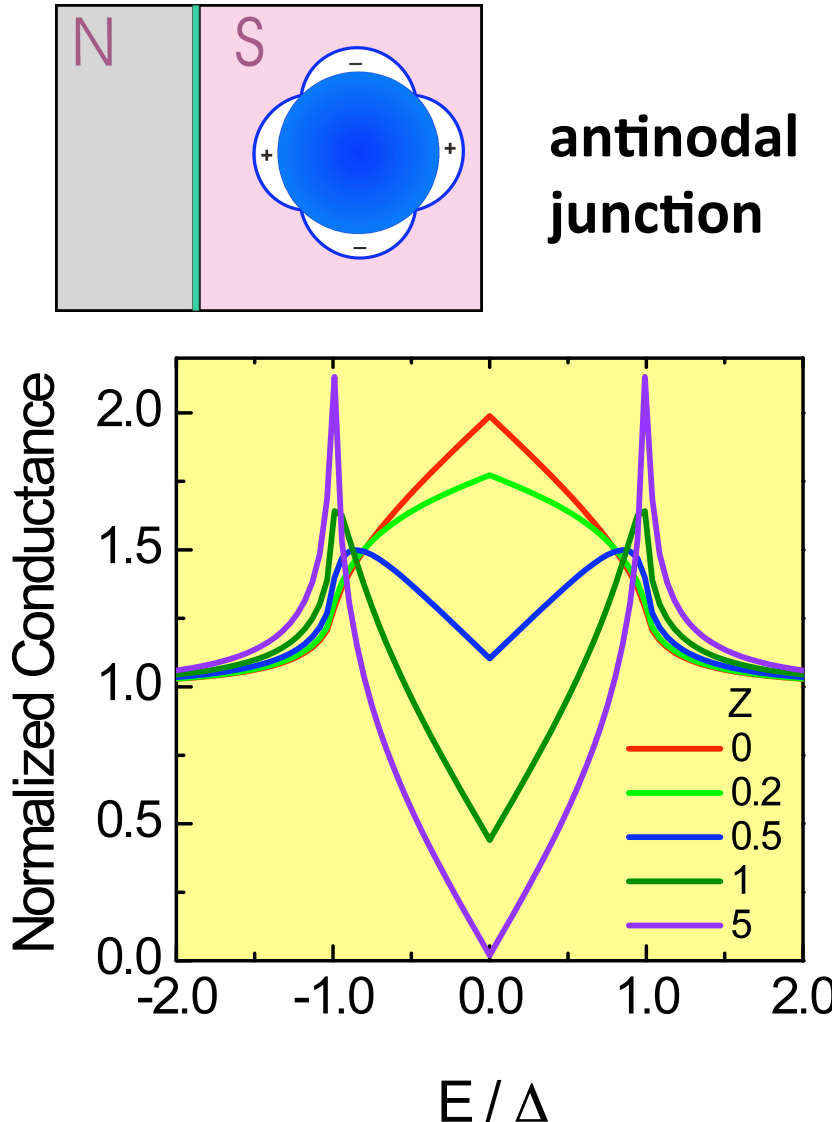


d-wave: nodal direction



YET AGAIN: d -wave BTK Model

Y. Tanaka et al. (PRL,1995) S.
Kashiwaya et al. (PRB,1996)



ABS Tunneling Spectroscopy of High- T_c Cuprates

VOLUME 79, NUMBER 2

PHYSICAL REVIEW LETTERS

14 JULY 1997

Observation of Surface-Induced Broken Time-Reversal Symmetry in $\text{YBa}_2\text{Cu}_3\text{O}_7$ Tunnel Junctions

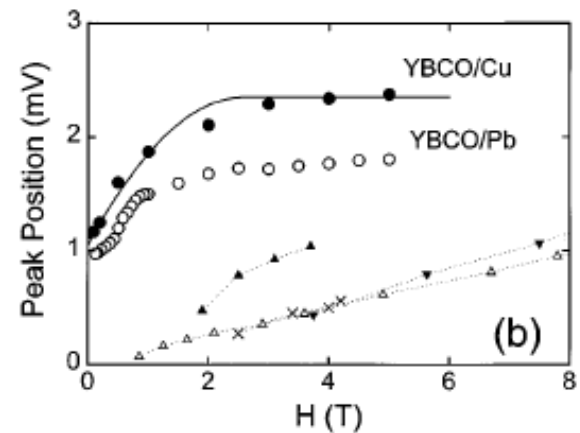
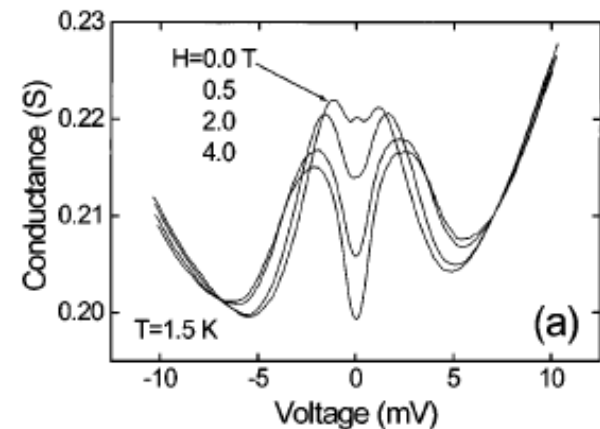
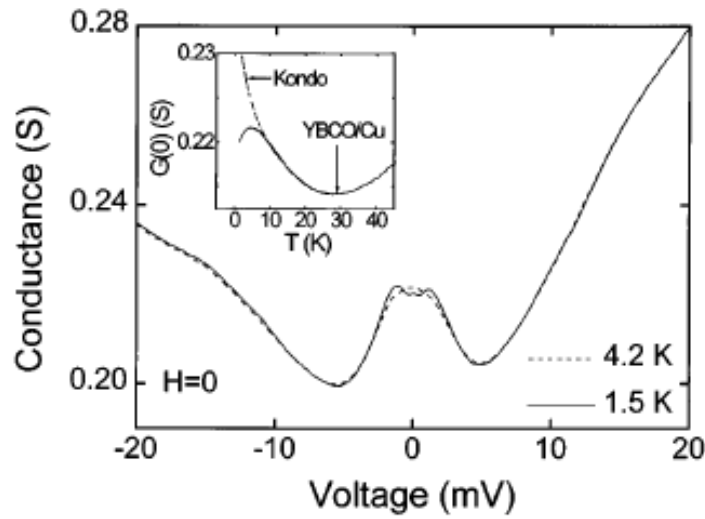
M. Covington,* M. Aprili, E. Paraoanu, and L. H. Greene

Department of Physics, University of Illinois at Urbana-Champaign, Urbana, Illinois 61801

F. Xu, J. Zhu, and C. A. Mirkin

Department of Chemistry, Northwestern University, Evanston, Illinois 60208

(Received 6 March 1997)



- ZBCP due to ABS splits under magnetic field (Doppler shift).

Further Extensions of BTK Model

- Mismatch in Fermi surface parameters
 - Fermi velocity \Rightarrow enhance Z_{eff}
 - Effective mass, Fermi wave vector \Rightarrow renormalized version of BTK
 - Fermi energy: breakdown of Andreev approximation ($\Delta \ll E_F$)
 \Rightarrow Imperfect retro-reflection

- Tunneling cone effect

Transmission Factor

$$D = A \exp(-2\kappa d / \cos \theta) = \exp\left(-\frac{\cos \theta_c}{\cos \theta_c - 1} \frac{\cos \theta - 1}{\cos \theta}\right) \quad \kappa = \left(\frac{2m}{\hbar^2}\right)^{1/2} [U - E]^{1/2}$$

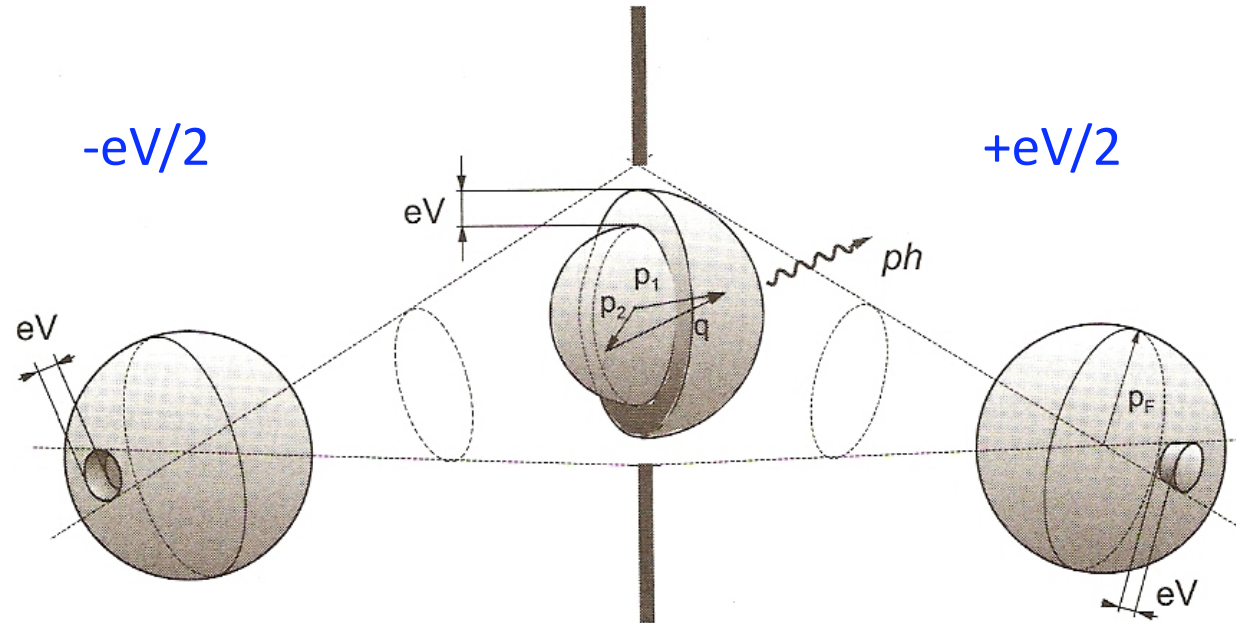
$$\theta_c = \cos^{-1}\left(\frac{2\kappa d}{1+2\kappa d}\right) = \cos^{-1}\left(\frac{1}{1+\frac{1}{2\kappa d}}\right) = \cos^{-1}\left(\frac{1}{1+\sqrt{\frac{1}{16\pi Z} \frac{d}{\lambda_F}}}\right)$$

$$Z = \frac{mH}{\hbar^2 k_F} = H / \hbar v_F$$

$$Z = \frac{m \cdot U \cdot d}{\hbar^2 k_F} = \frac{2m \cdot U}{\hbar^2} \frac{d}{2k_F} = \kappa^2 \frac{d}{2k_F}$$

$$\Rightarrow \kappa = \sqrt{\frac{2k_F Z}{d}}, \kappa d = \sqrt{2k_F d Z} = \sqrt{4\pi Z \frac{d}{\lambda_F}}$$

What is Point-Contact Spectroscopy (PCS) ?



- If two bulk metals are in contact with each other and the contact size is smaller than electronic mean free paths, quasiparticle energy gain/loss mostly occurs at the constriction.
- Nonlinearities in current-voltage characteristics reflect energy-dependent quasiparticle scatterings in the contact region.

Junction Size Matters in PCS!

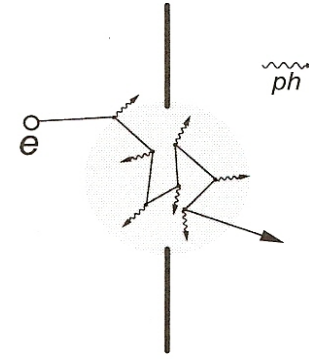
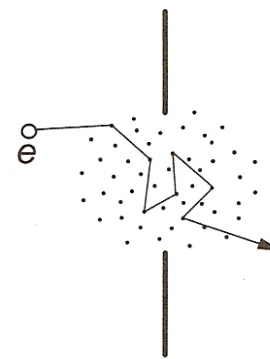
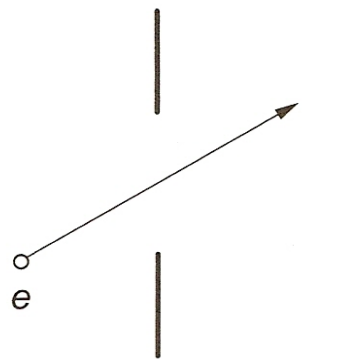
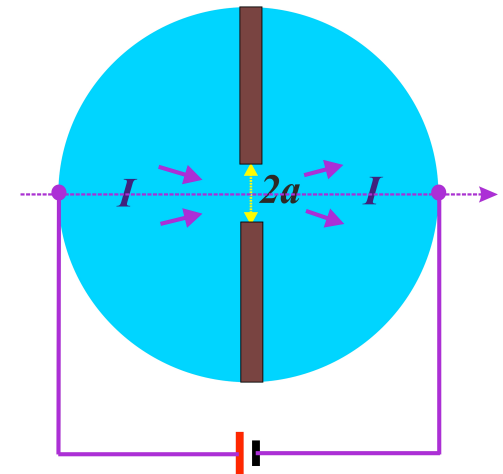
Wexler's formula

G. Wexler, Proc. Phys. Soc. London **89**, 927 (1966)

$$R_0 = \frac{4\rho l_{el}}{3\pi a^2} \left\{ 1 + \frac{3\pi}{8K} \gamma(K) \right\}, \quad K \equiv l_{el}/a, \text{ Knudsen ratio}$$

i) $K \gg 1$, $\gamma(K) \rightarrow 0.694$, $R_0 = \frac{4\rho l_{el}}{3\pi a^2}$, Sharvin limit

ii) $K \rightarrow 0$, $\gamma(K) \rightarrow 1$, $R_0 = \frac{\rho}{2a}$, Maxwell limit



Ballistic

Diffusive

Thermal

$$l_{el}, l_{in}$$

$$\sqrt{l_{el} \cdot l_{in}}$$

Contact
Size d

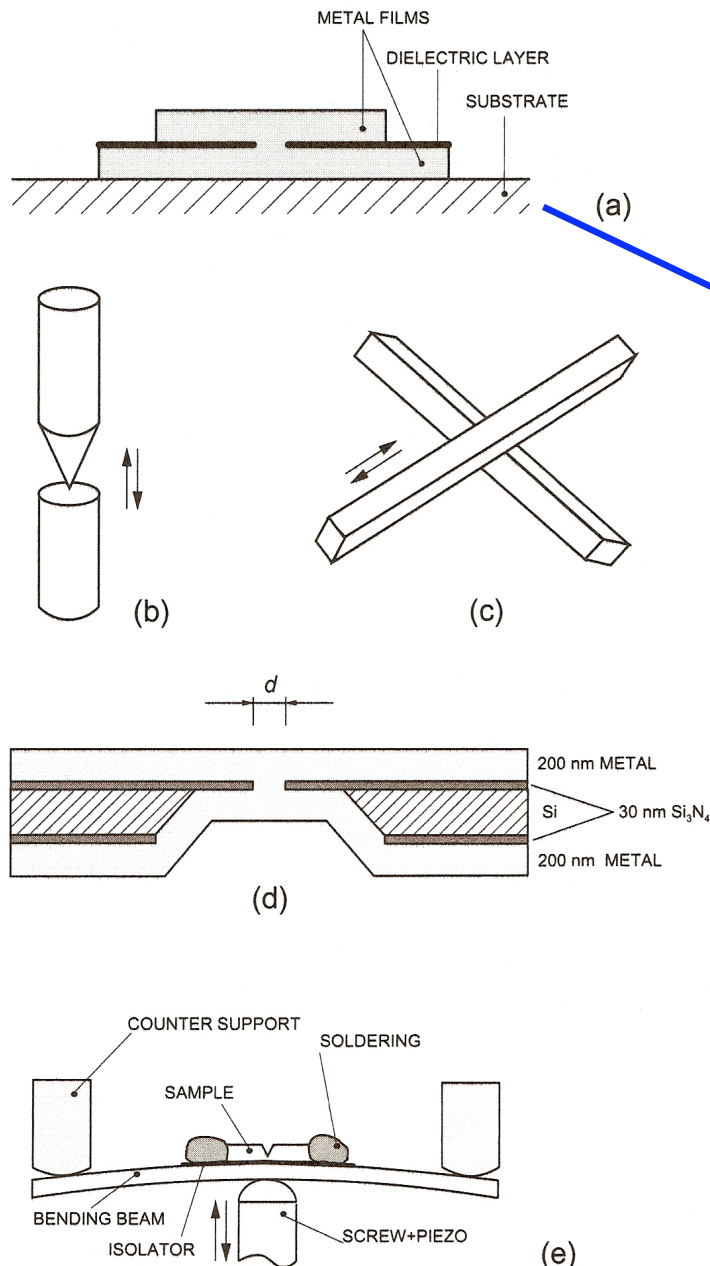
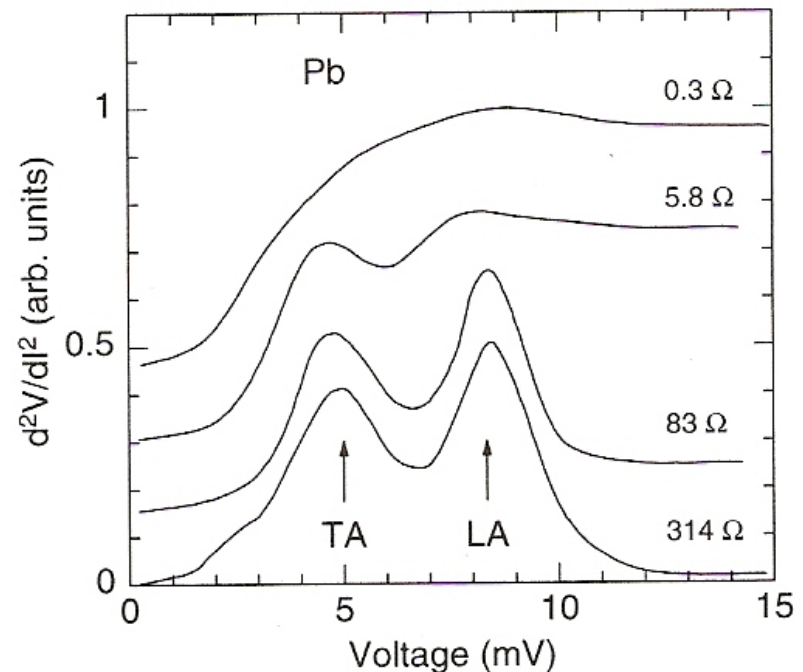


Fig. 4.1. Schematic view of different methods of point-contact formation: (a) thin films, (b) needle-anvil, (c) shear, (d) lithography, and (e) break-junction (see text for details).

Point Contact Techniques

I K Yanson

Sov. Phys. JETP 39,
506 (1974)



$$\frac{d^2V}{dI^2} \propto \alpha(\omega)^2 F(\omega)$$

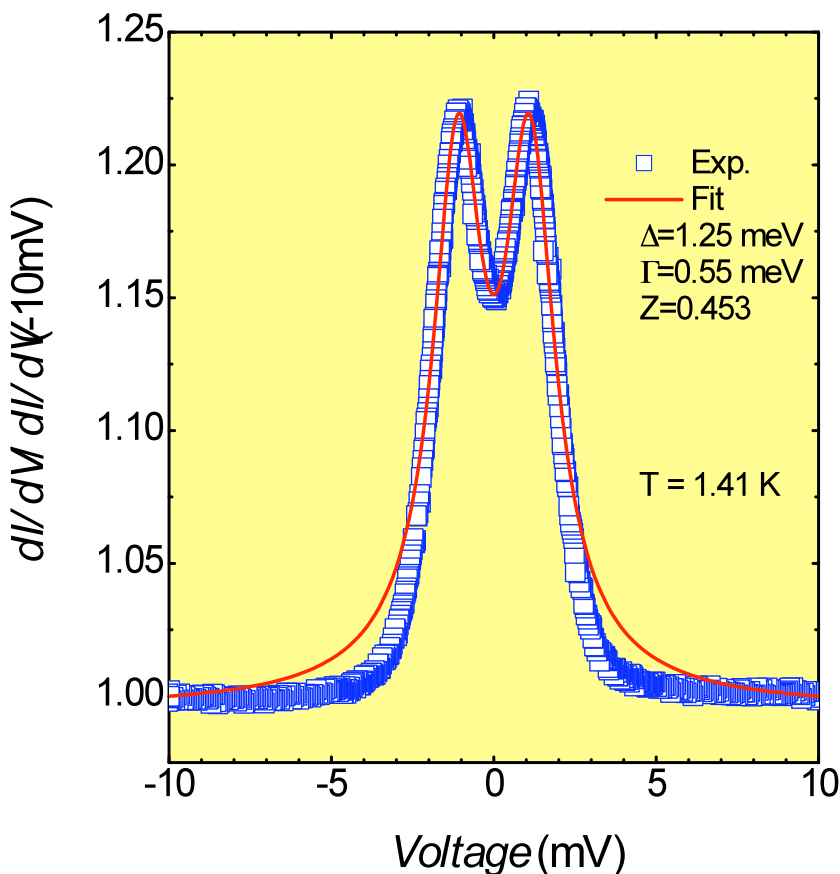
Similar to tunneling results by McMillan and Rowell (1965)

Needle-anvil tech. developed by
A.G.M. Jansen *et al.*

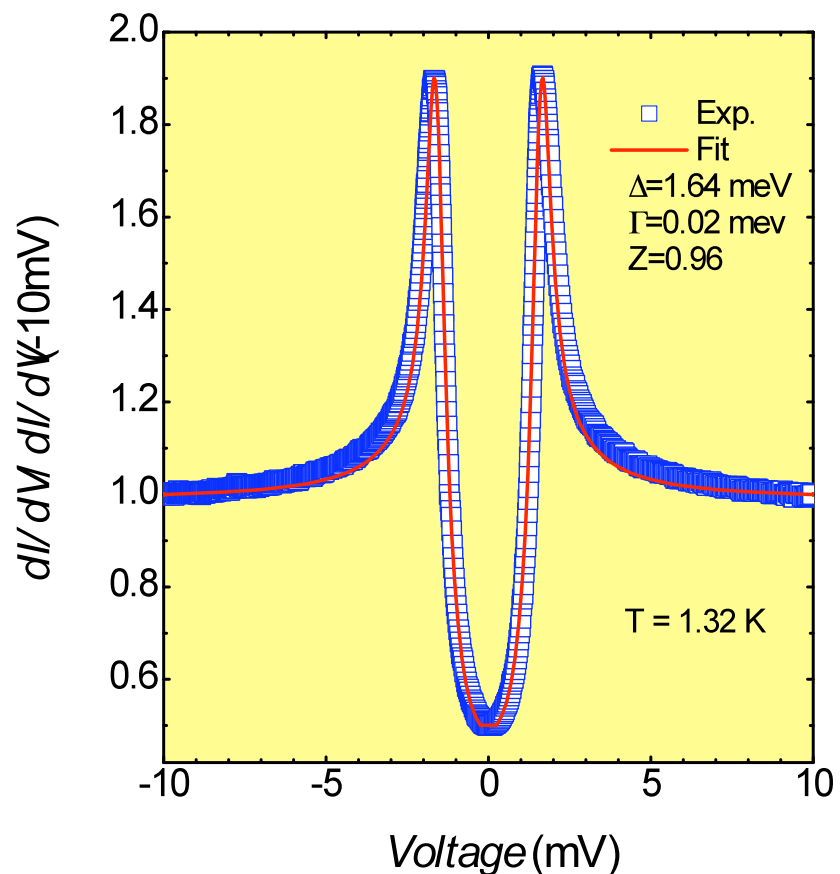
Example (I): Au/Nb

Park & Greene, *Rev. Sci. Instum.* **77**,
023905 (2006)

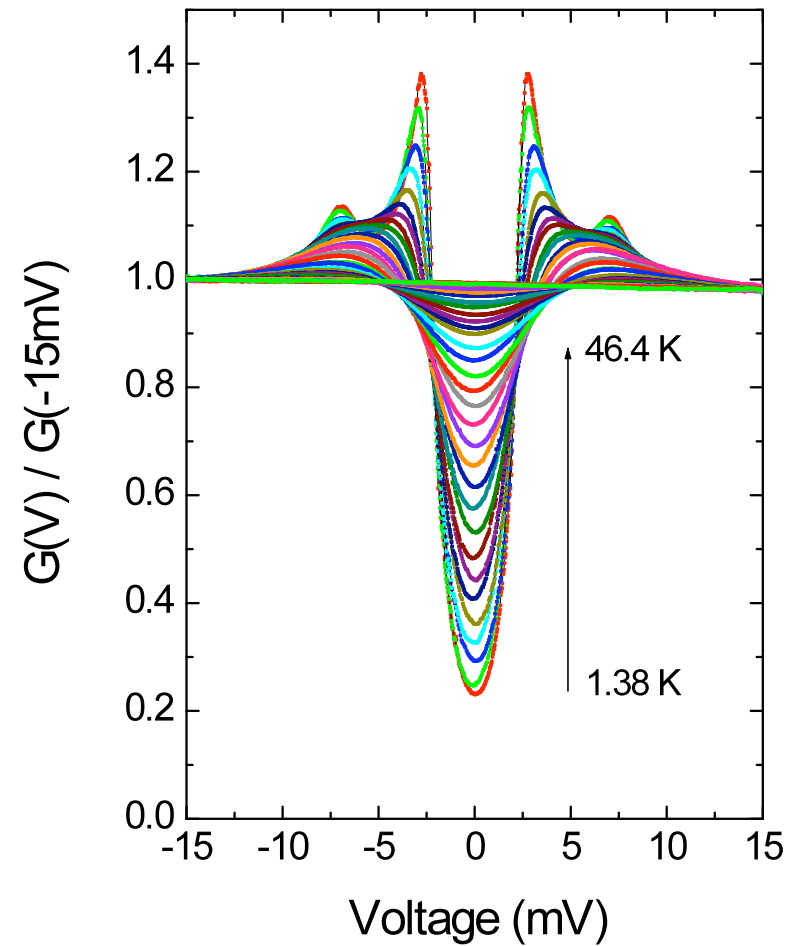
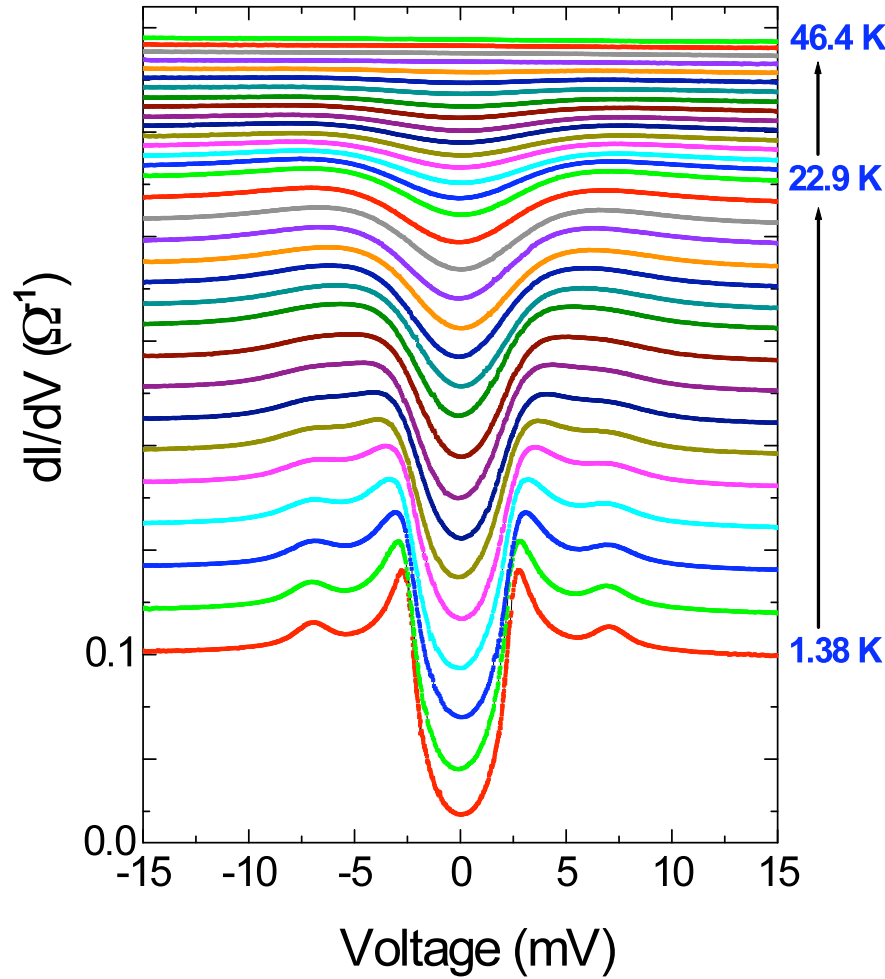
$$\frac{dI}{dV} \propto \int_{-\infty}^{\infty} \frac{\partial f(E - eV)}{\partial(eV)} [1 + aa^* - bb^*] dE$$



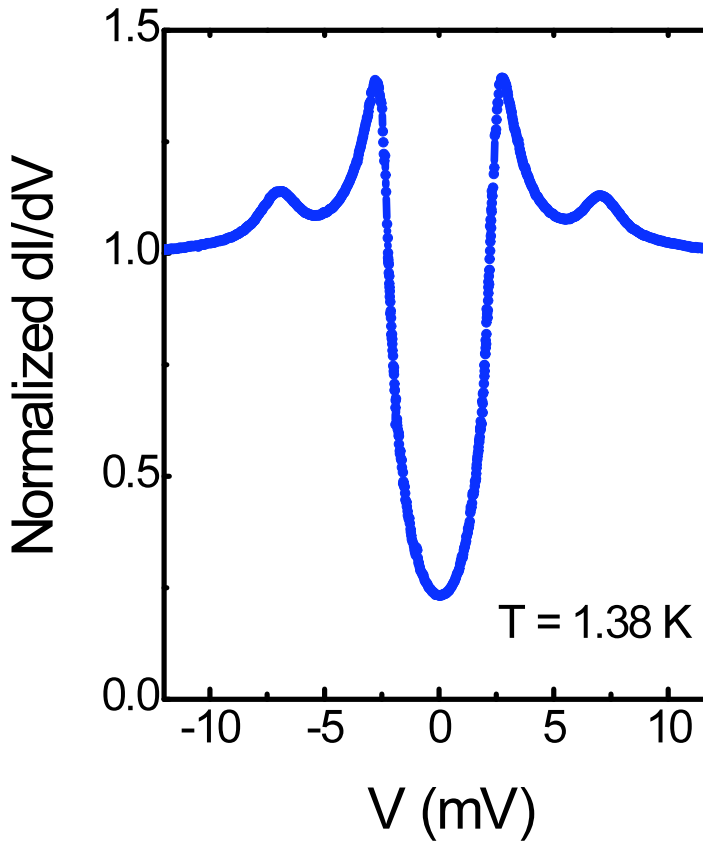
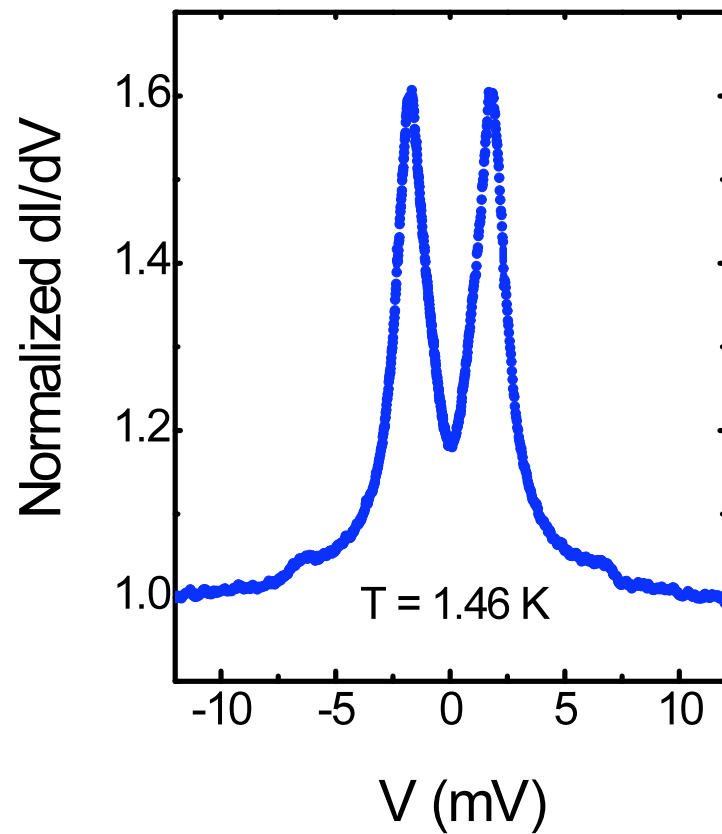
Δ : Energy gap
 Γ : Quasiparticle smearing
Z : Tunnel barrier strength



Example (II): Au/MgB₂



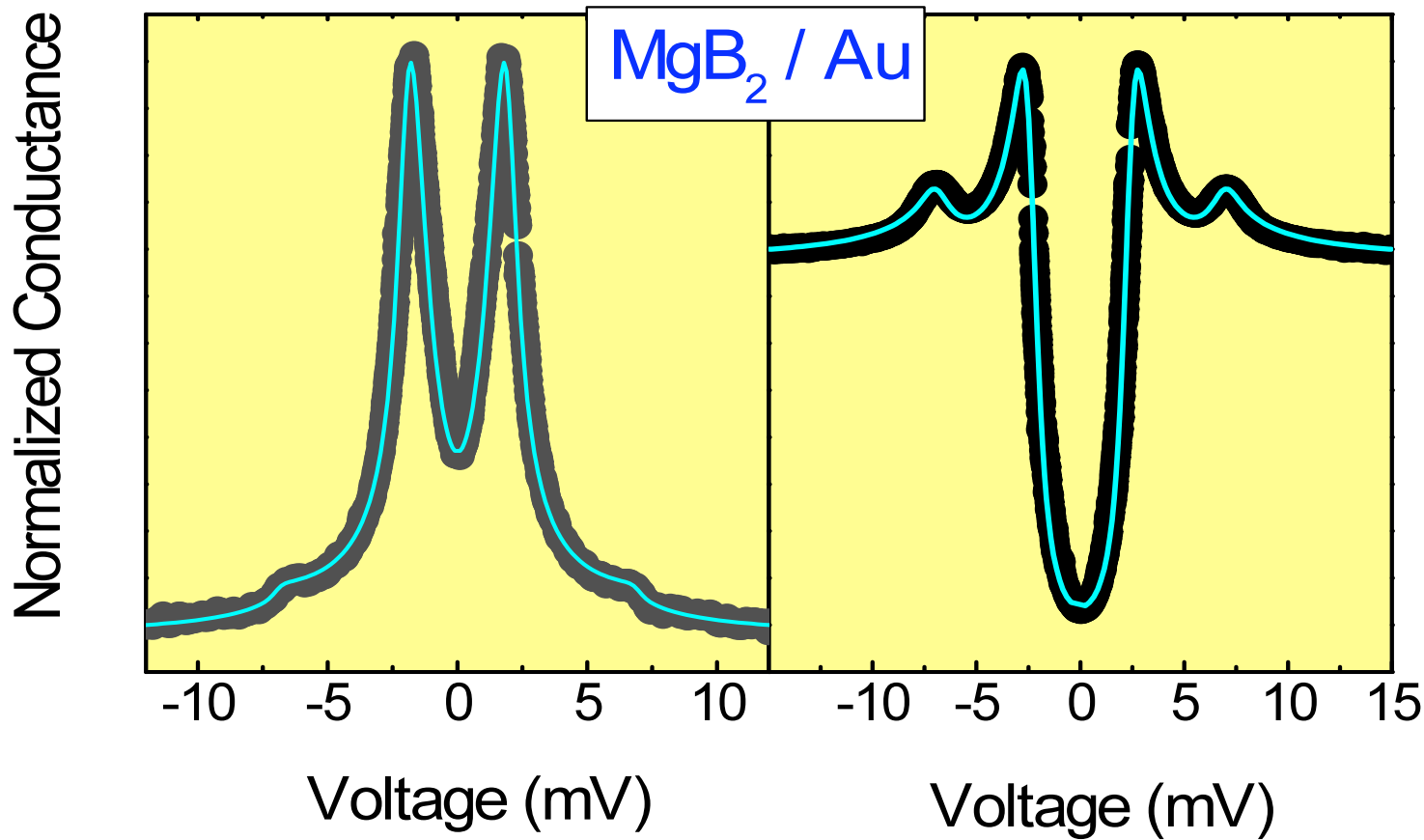
Two types of conductance curves from MgB₂/Au



Two-band BTK model

$$\frac{dI}{dV} = \omega_\pi \left. \frac{dI}{dV} \right|_\pi + (1 - \omega_\pi) \left. \frac{dI}{dV} \right|_\sigma$$

$$\left. \frac{dI}{dV} \right|_i = \int_{-\infty}^{\infty} dE [1 + A(E, \Gamma, Z) - B(E, \Gamma, Z)] \frac{\partial f(E - eV, T)}{\partial (eV)}$$



$$\Delta = 1.97, 6.90 \text{ meV}$$

$$\Gamma = 0.18, 0.01 \text{ meV}$$

$$Z = 0.47, 0.25$$

$$\omega_\pi = 0.972$$

$$\Delta = 2.43, 7.00 \text{ meV}$$

$$\Gamma = 0.41, 0.45 \text{ meV}$$

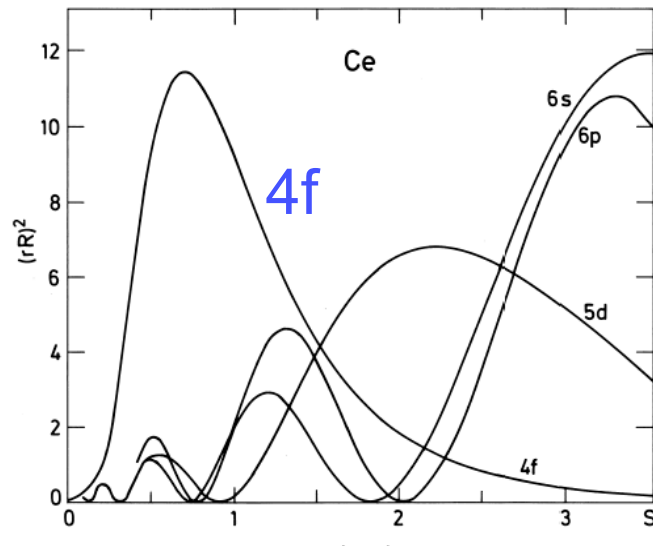
$$Z = 2.5, 0.9$$

$$\omega_\pi = 0.90$$

Conclusions for BTK Model

- Blonder-Tinkham-Klapwijk (BTK) theory can explain the transitional behavior **from Andreev reflection to Tunneling** using a single parameter, the effective barrier strength (**Z**).
- BTK and extended BTK theories provide a useful framework to understand charge transport phenomena in various types of N/S hetero-structures.
- To analyze PCS data on a superconductor using BTK theory, three fitting parameters: Z , Δ , Γ
- BTK theory has been successfully applied to analyze our PCS data for Nb and MgB_2 .

1-1-5 Heavy-Fermion Compounds



Periodic Table of the Elements

mass → 12.011	-4	← Selected Oxidation States
symbol → C	+2	
atomic number → 6	+4	
stable isotope → 12	2-4	

Relative atomic masses are based on $^{12}\text{C} = 12.000$

Note: Mass numbers in parentheses are mass numbers of the most stable or common isotope.

Group		13	14	15	16	17	18
B	C	N	O	F	Ne		
Al	Si	P	S	Cl	Ar		
Ga	Ge	As	Se	Br	Kr		
In	Sn	Sb	Te	I	Xe		
Ru	Rh	Pt	Au	Hg	Tl	Pb	At
Tc	Ag	Ir	Pd			Bi	Po
Mo	45	46	47	48	49	50	51
42	43	44	45	46	47	48	49
101.07	102.18	103.18	104.18	105.18	106.18	107.18	108.18
183.85	186.37	190.2	192.22	195.89	196.967	200.54	204.24
144.008	144.24	145	150.36	151.16	157.25	158.025	162.50
144.008	144.24	145	150.36	151.16	157.25	158.025	162.50
Th	Pa	U	Np	Pu	Am	Cm	Bk
90	91	92	93	94	95	96	97

*The systematic names and symbols for elements of atomic numbers above 109 will be used until the approval of trivial names by IUPAC.

**Denotes the presence of (2-8-) for elements 72 and above
Ce
Pr
Nd
Pm
Sm
Eu
Gd
Tb
Dy
Ho
Er
Tm
Yb
Lu
Th
Pa
U
Np
Pu
Am
Cm
Bk
Cf
Es
Fm
Md
No
Lr

4f or 5f electrons



CeMIn_5

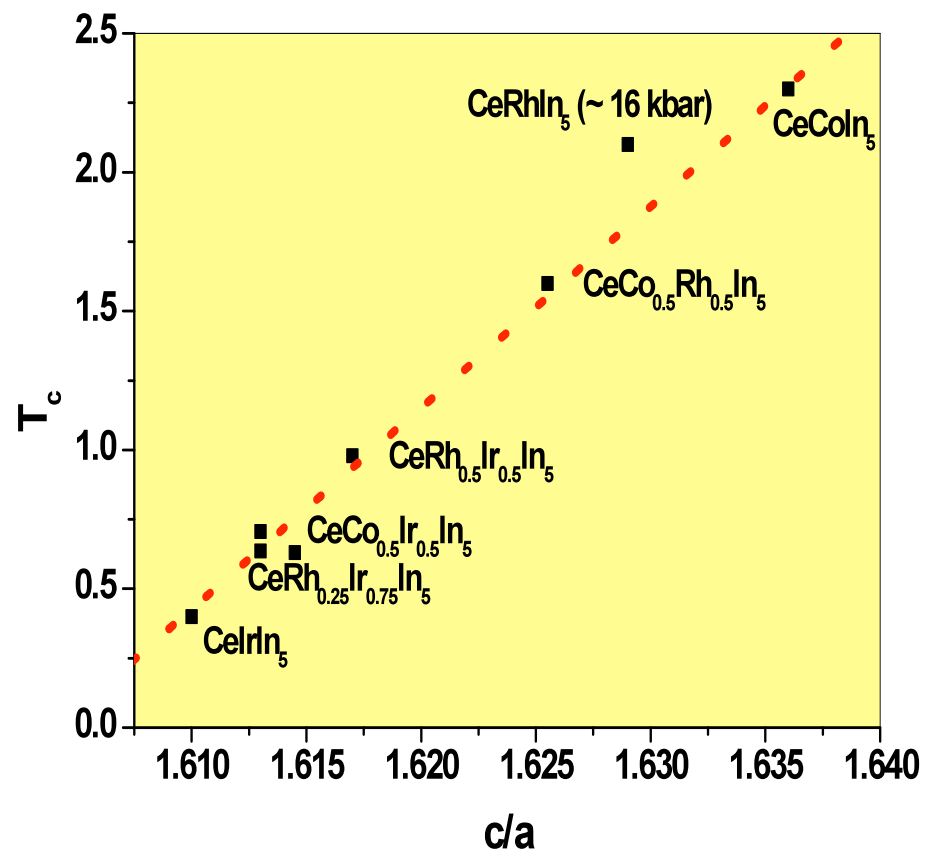
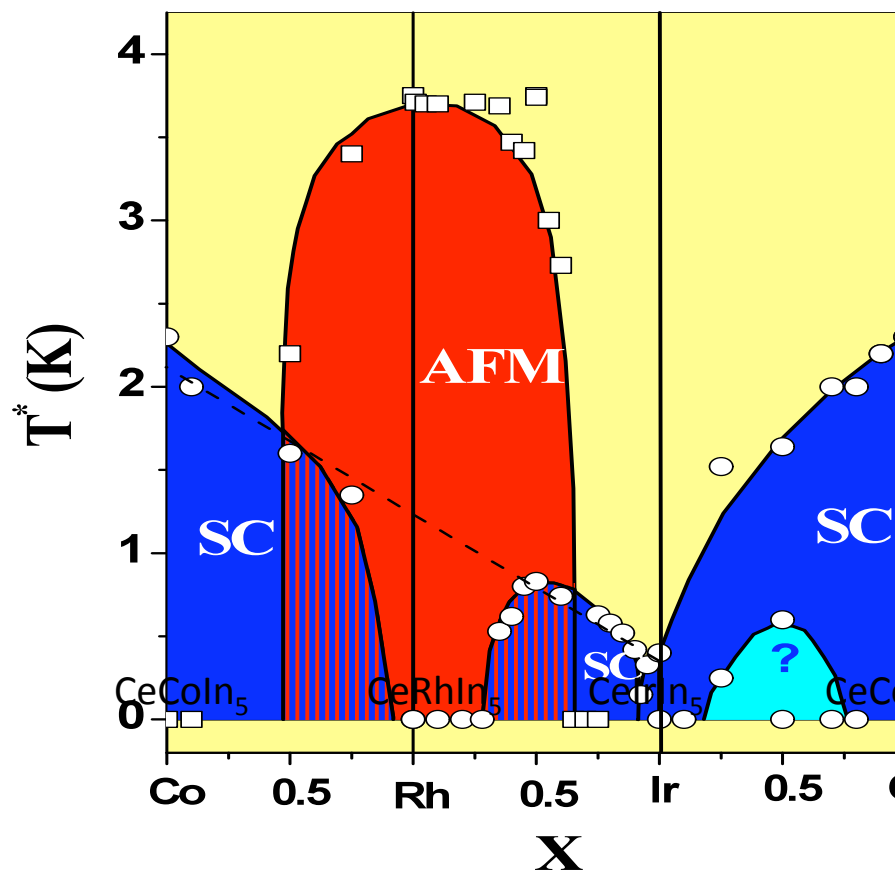
CeCoIn_5 ($T_c=2.3 \text{ K}$, $g_{\text{el}}=290 \text{ mJmol}^{-1}\text{K}^{-2}$)

PuMGa_5

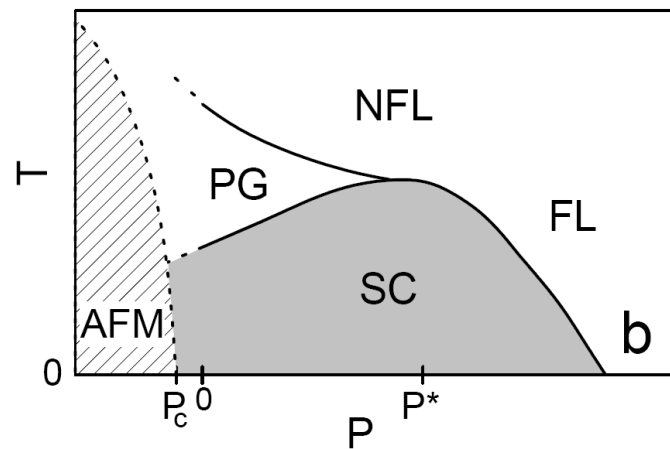
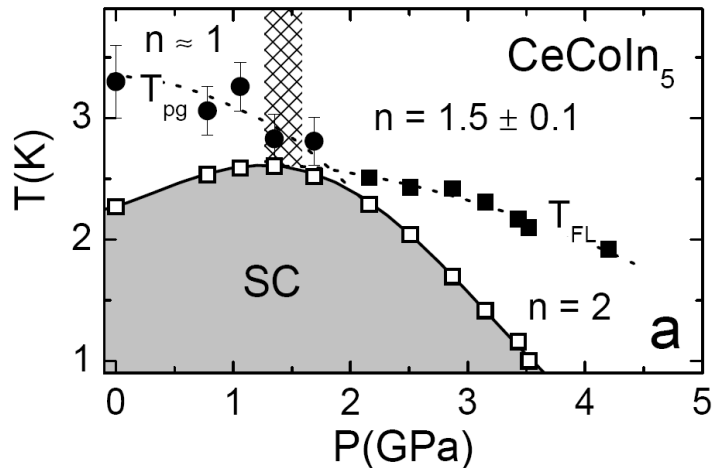
PuCoGa_5 ($T_c=18.5 \text{ K}$, $g_{\text{el}}=77 \text{ mJmol}^{-1}\text{K}^{-2}$)

The Heavy Fermion Superconductor CeColn₅:

Phase diagram of series Ce M In₅ (M = Co, Rh, Ir)



The heavy-fermion Superconductor CeCoIn₅: Some interesting properties



V. A. Sidorov et al.,
PRL 89, 157004 (2002)

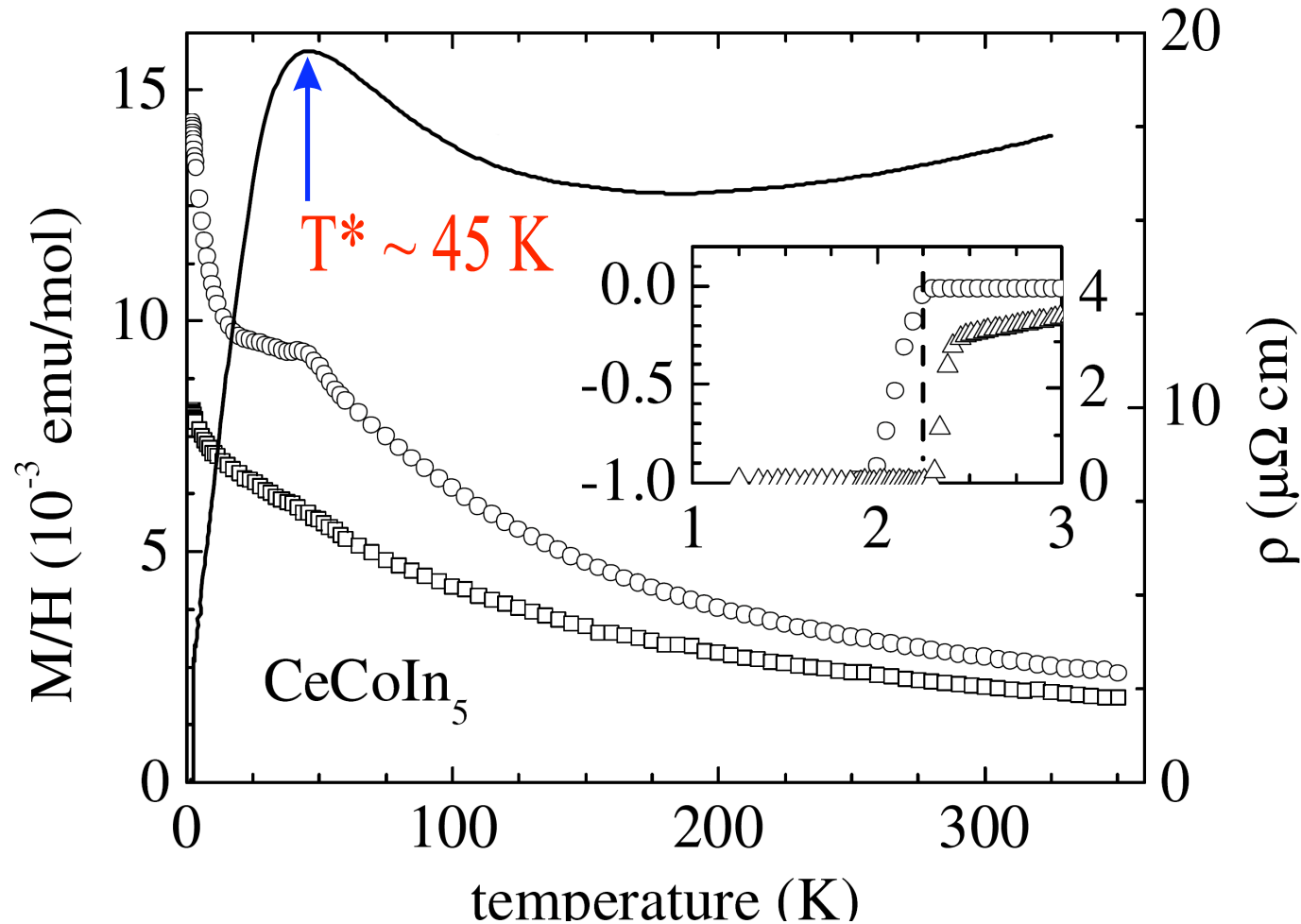
- Quantum Phase Transition with chemical substitution, hydrostatic pressure, magnetic field , (similar to cuprates)
- FFLO Phase Transition

➤ Anisotropic type-II SC
 ➤ Heavy-fermion liquid
 $m_{\text{eff}} = 83m_0$
 $T^* \sim 45 \text{ K}$
 ➤ Non-Fermi liquid
 $\rho \sim T^{1.0 \pm 0.1},$
 $C_{\text{en}} / T \sim -\ln T,$
 $1 / T_1 T \sim T^{-3/4}$

The Heavy-Fermion Superconductor CeCoIn₅

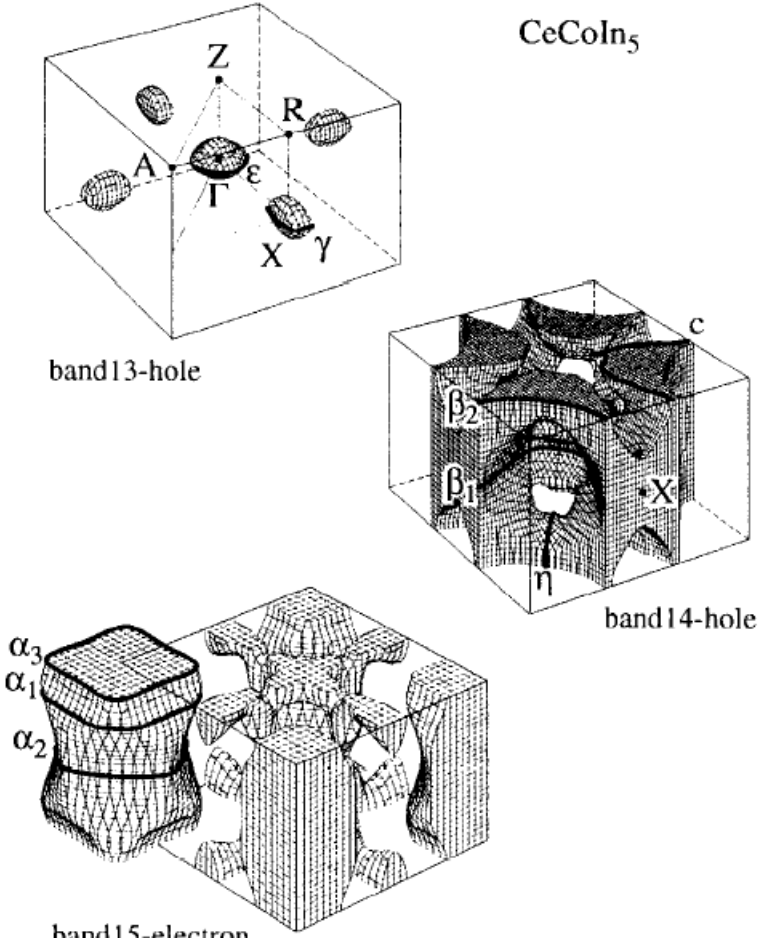
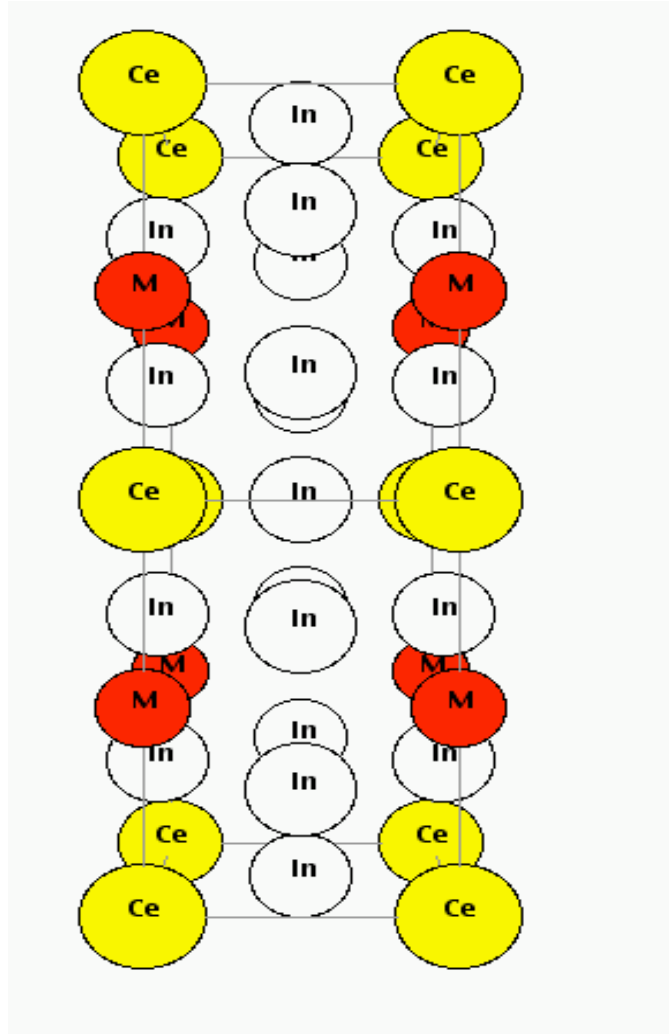
Why it is our HFS of choice (ideal for PCS):

- $T_c = 2.3\text{K}$ (high for HFS)
- Superconductivity in clean limit ($mfp = 810\text{\AA} \gg \xi_0$)



C. Petrovic *et al.*, J. Phys.: Condens. Matter **13**, L337 (2001)

Crystal Structure and Fermi Surface: Quasi 2-dimensional



R. Settai et al., JPCM **13**, L627 (2001)

BTK model has worked well for a wide range of materials, but as we will see, NOT for heavy-fermion superconductor / normal metal (HFS/N) interfaces

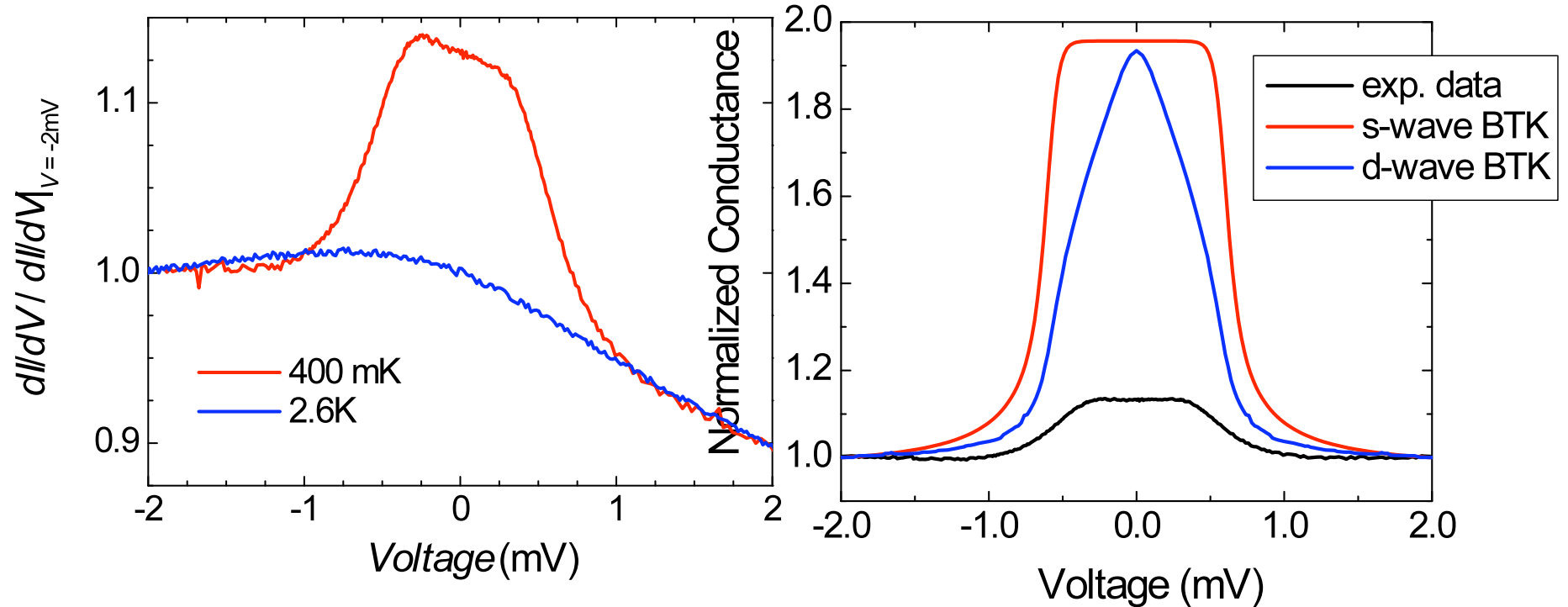
The Fermi velocity mismatch is so great at the HFS/N interface that Andreev reflection (AR) should never occur ($Z>5 \rightarrow$ expect the extreme tunneling limit).

Recall effective barrier strength: $Z_{eff} = \sqrt{Z^2 + \frac{(1-r)^2}{4r}}, r \equiv \frac{v_{FN}}{v_{FS}}$

However, AR is routinely measured at the N/HFS interface, albeit suppressed compared to N/conventional-S.

Andreev reflection at the N/HFS interface cannot be explained by existing theories

Definition of the issues



1. Understanding charge transport across HF interface

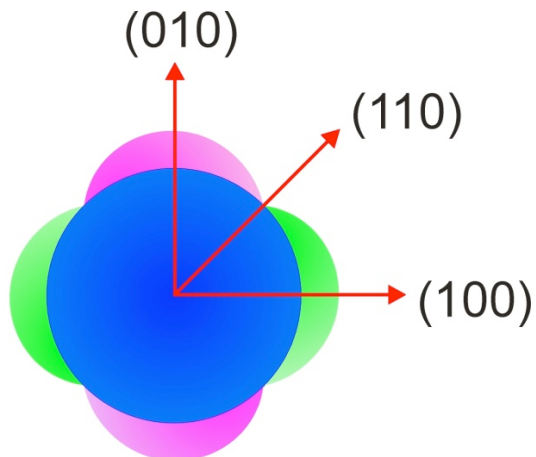
Existing models cannot account for
Andreev reflection at the HFS/N interface

2. Spectroscopic studies of CeCoIn_5 (OP symmetry, mechanism,...)

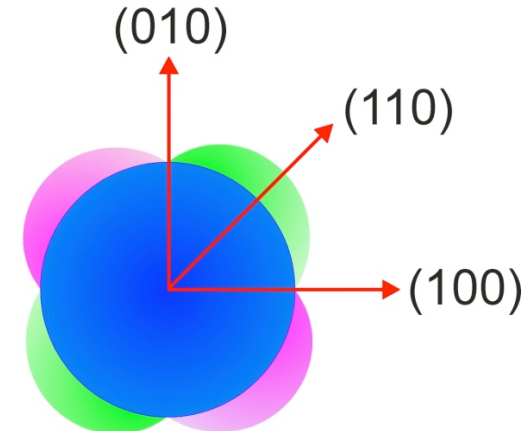
The “Rosetta stone for heavy fermions”

CeCoIn₅: Superconducting Order Parameter Symmetry: Previous work

- Evidence for the existence of line nodes:
Power law dep: $C_{\text{en}} / T \sim T$, $\kappa \sim T^{3.37}$, $1/T_1 \sim T^{3+\epsilon}$, $\lambda \sim T^{1.5}$
- Four-fold symmetry of field-angle dep in thermal cond.:
small angle neutron scattering $\Rightarrow d_{x^2-y^2}$
specific heat $\Rightarrow d_{xy}$
- Spectroscopic evidence was lacking to determine the locations of line nodes: (110) or (100) i.e. d_{xy} or $d_{x^2-y^2}$?



$$d_{x^2-y^2}$$



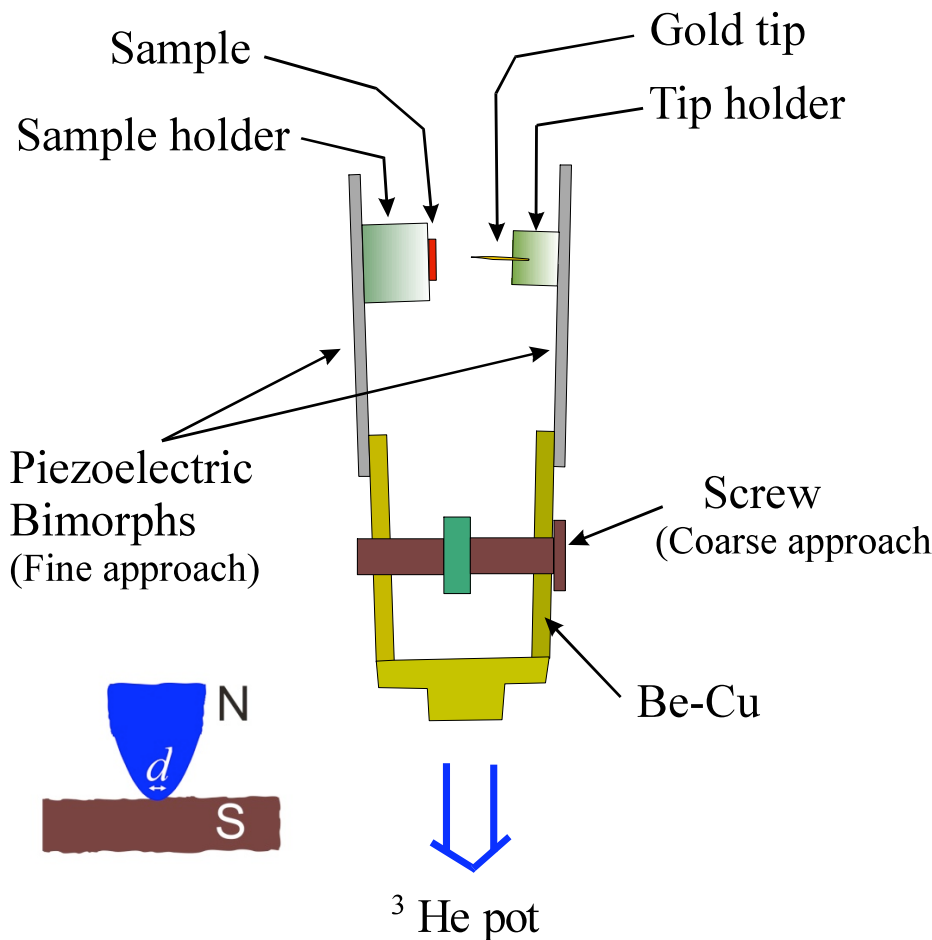
$$d_{xy}$$

Our Experiments:

Point Contact Andreev Reflection Spectroscopy (PCARS)

1) Cantilever-Andreev-Tunneling (CAT) Rig

W.K. Park, LHG, RSI (06).



Gold tip

- electrochemically etched
- CeCoIn₅ single crystal
- (001), (110) and (100) oriented
- etch-cleaned using H₃PO₄

Coarse approach

- done before inserting probe

Fine approach

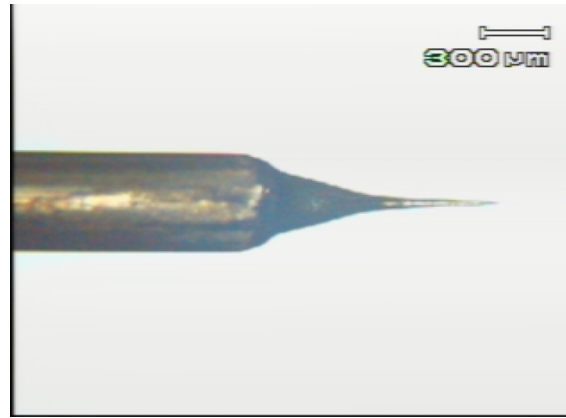
- done during cool down
- piezo driven by computer control

Operation range

- Temperature : down to 300mK
- Magnetic Field : up to 12T

Basics of PCS: Tip production

The sharp gold tip is electrochemically etched in hydrochloric acid

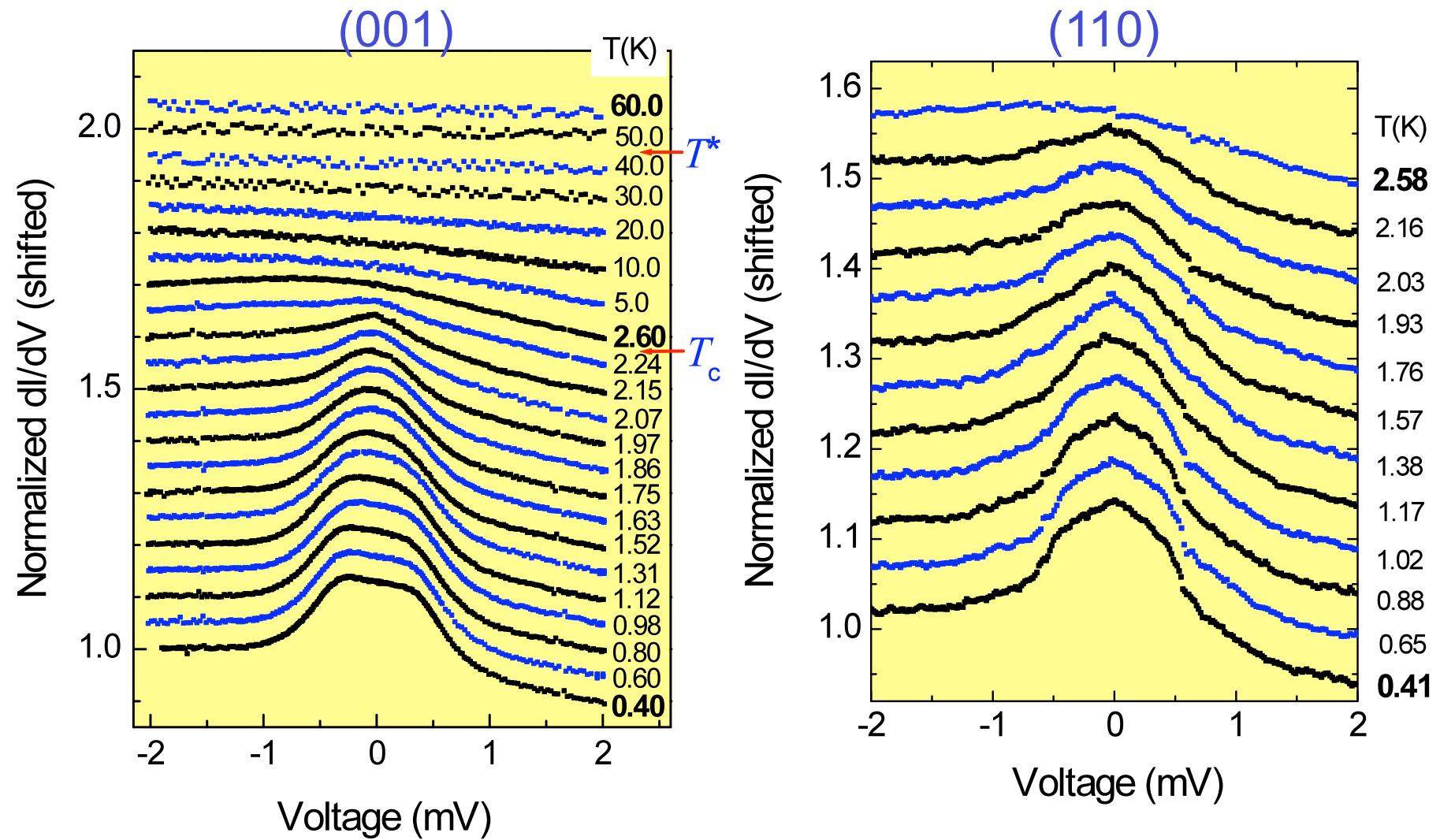


For our experiment ($R_N = 1\text{-}4 \Omega$) and not T-dep:

- * Upper limit of $2a = 46 \text{ nm}$
- * I_{el} at $T_c =$ is 81 nm (from thermal conductivity),
and increases with decreasing T , to $4\text{-}5 \mu\text{m}$ at 400mK .

**Our experiments are in the Sharvin Limit,
and are reproducible.**

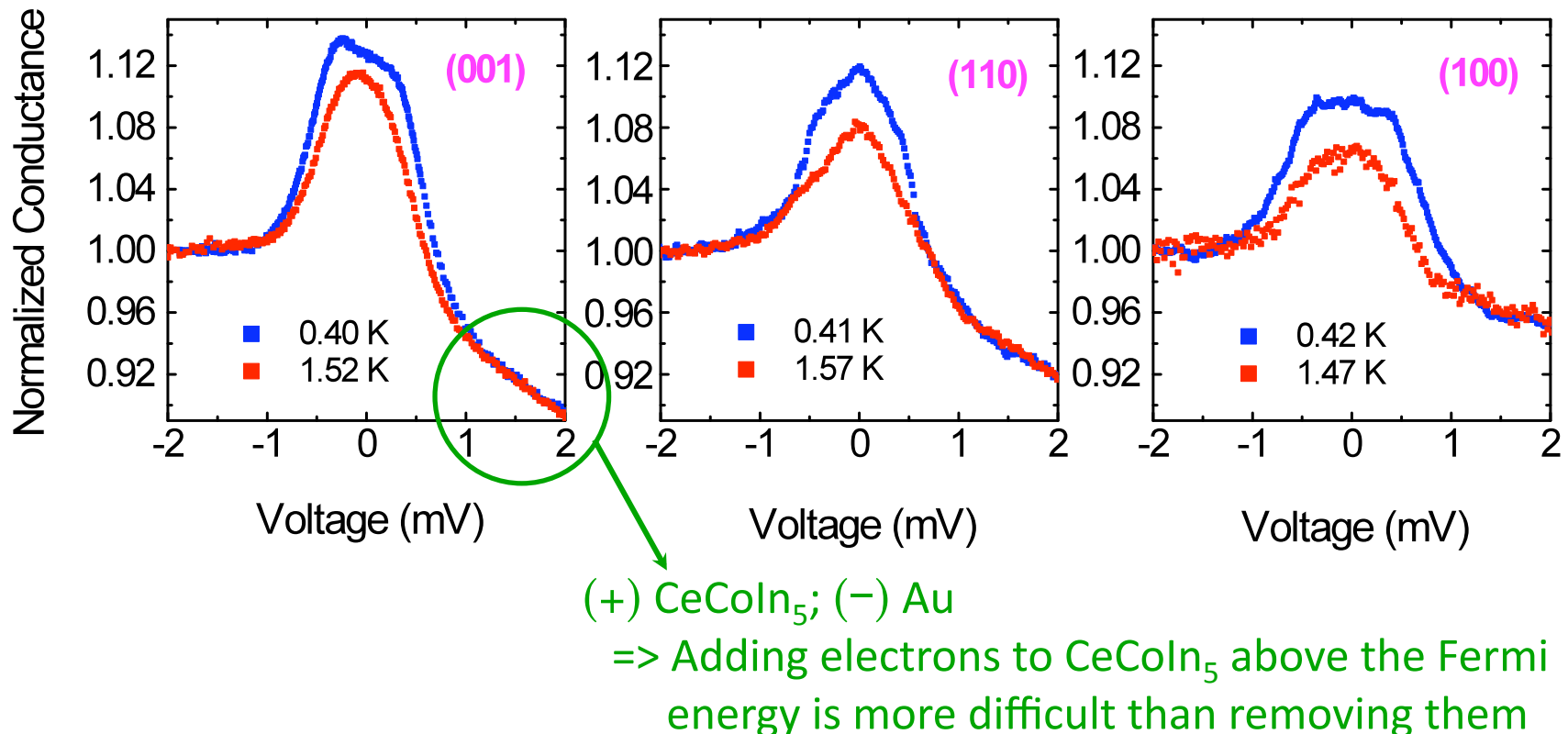
Andreev Reflection Conductance of Au/CeCoIn₅



Conductance asymmetry begins at T^* and saturates below T_c

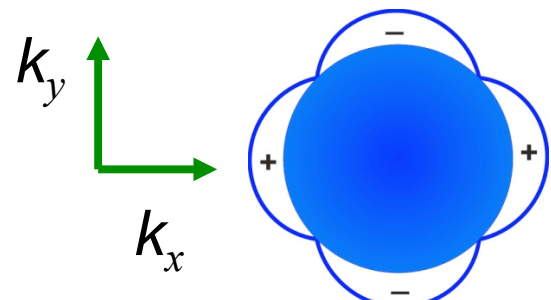
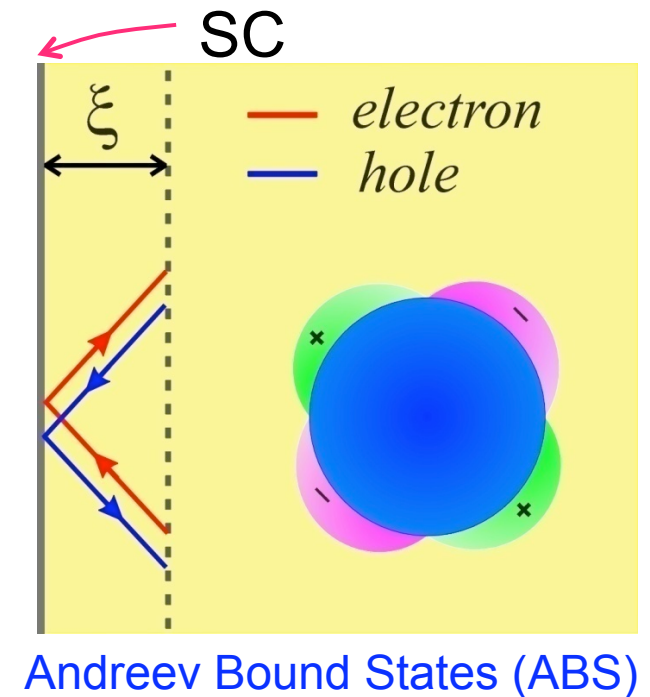
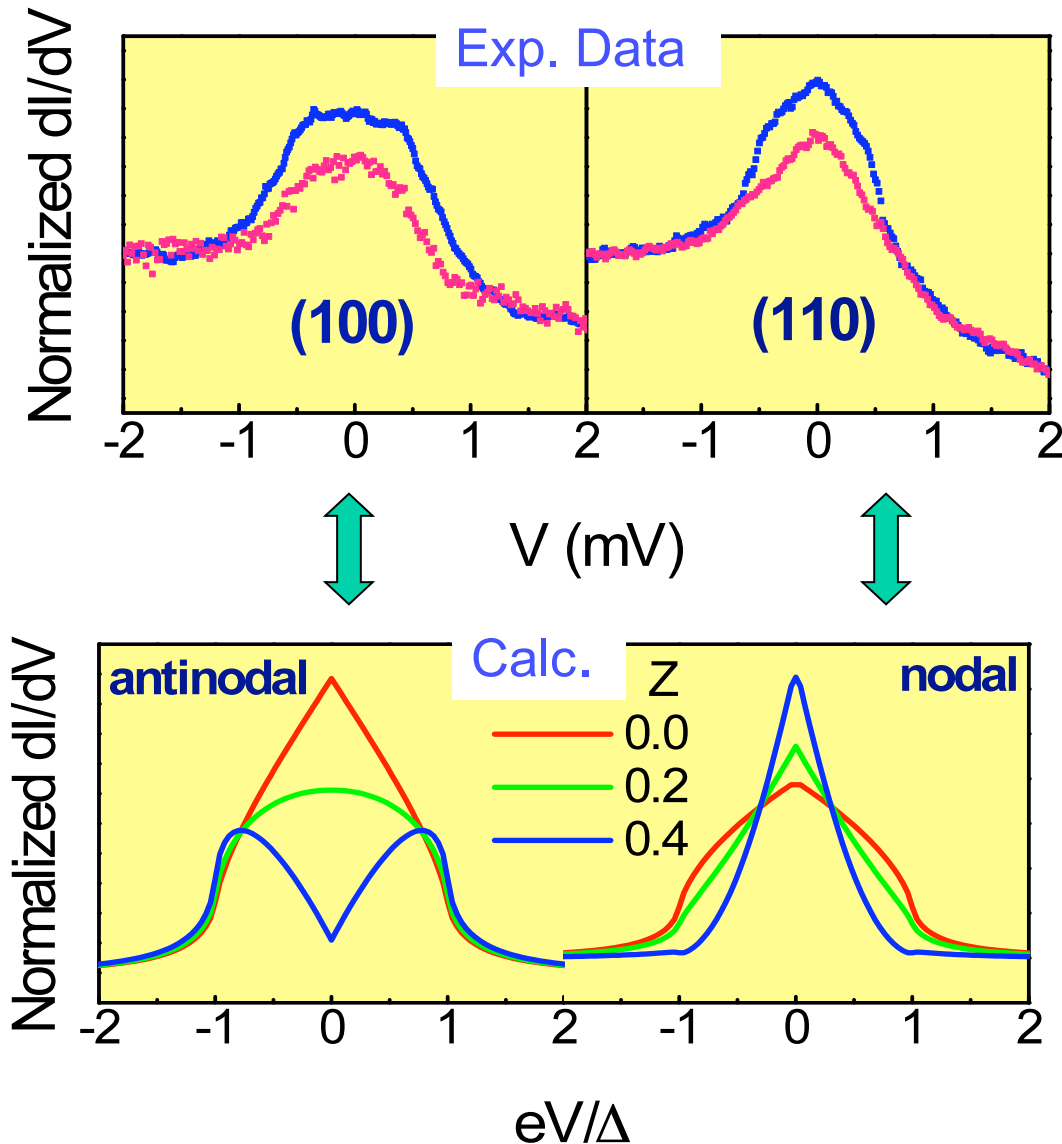
Consistency Along Three Orientations

- Conductance magnitude (AR)
- Conductance width (Δ)
- Background asymmetry (2-fluid & DoS peak ?)



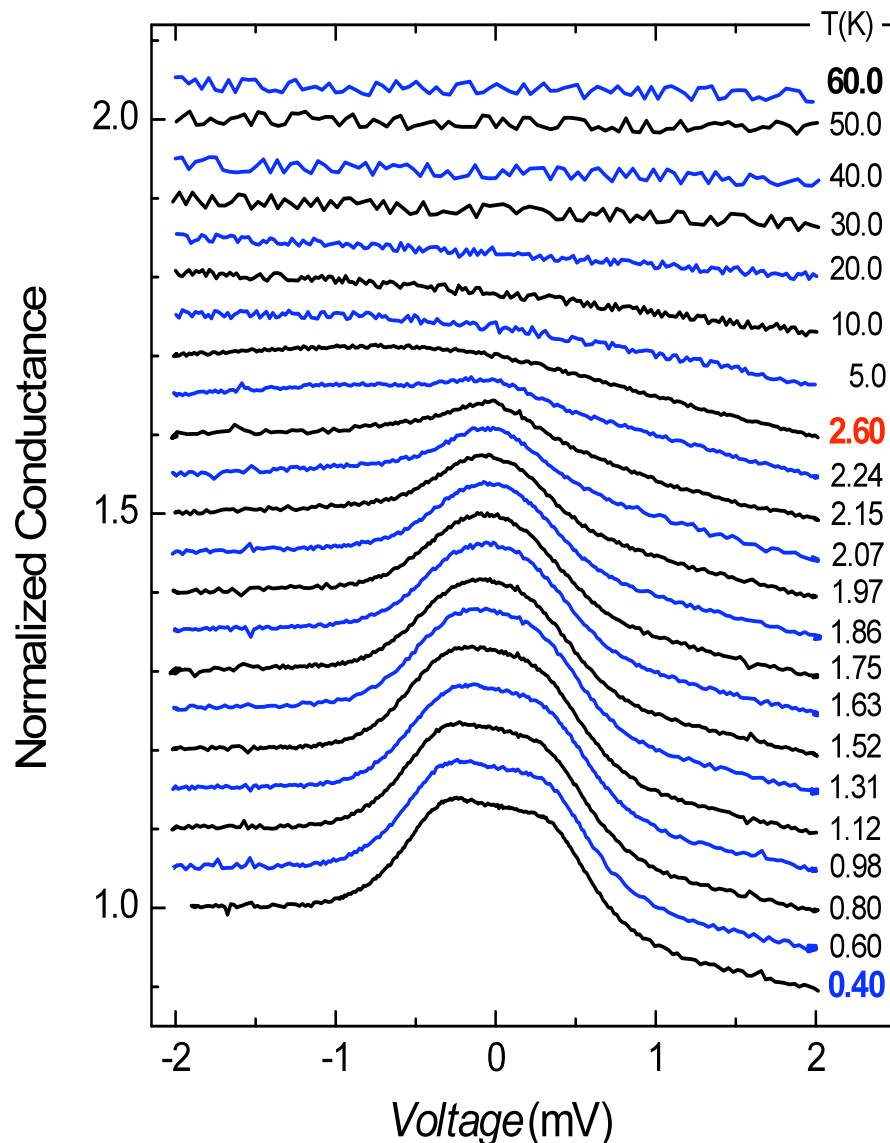
Note the shapes of the conductance curves

Spectroscopic Evidence for $d_{x^2-y^2}$ Symmetry



WKP et al., PRL 100, 177001 (2008)

Background Conductance Asymmetry of Au/CeCoIn₅

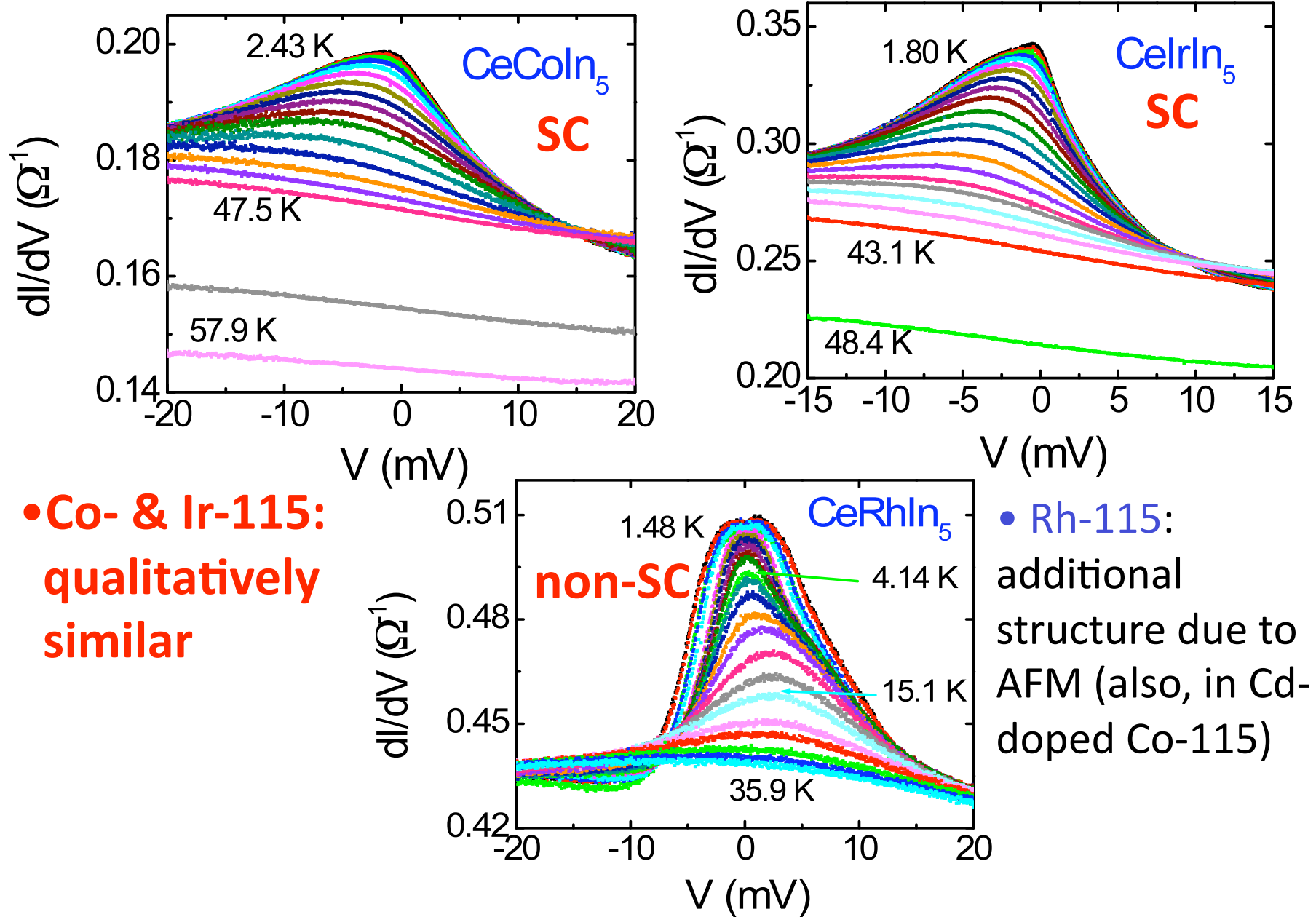


T^* Background develops an **asymmetry*** at the heavy-fermion liquid coherence temperature,
 $T^* \sim 45$ K.

T_c This asymmetry gradually increases with decreasing temperature until the onset of superconducting coherence,
 $T_c = 2.3$ K.

* el-h asymmetry described by Nakatsuji, Pines & Fisk, PRL 92, 016401 (2004)

Background Conductance Asymmetry of Au/CeMIn₅

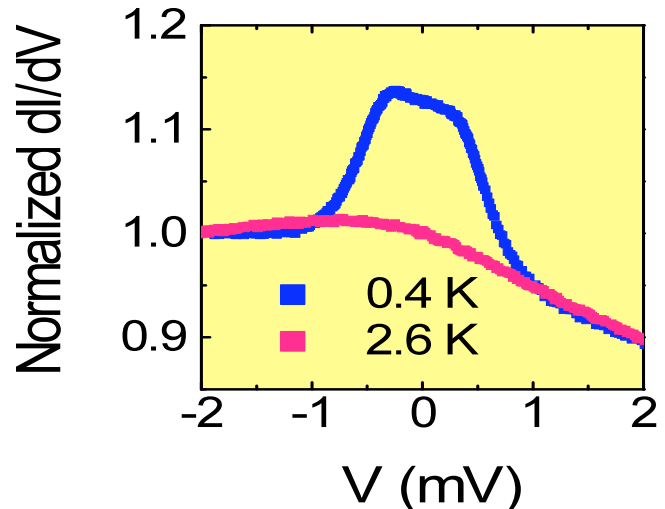


Why is the conductance asymmetric?

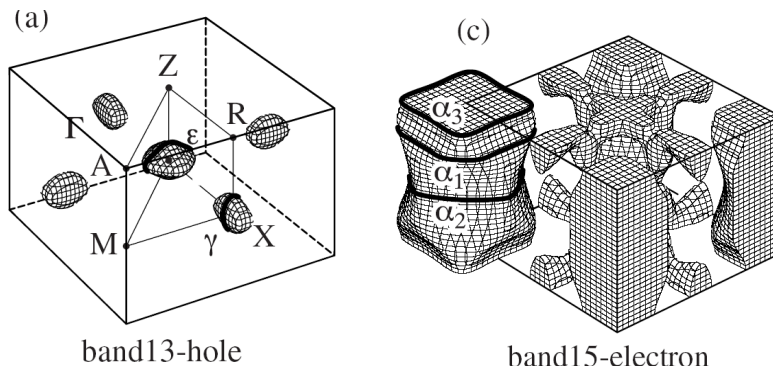
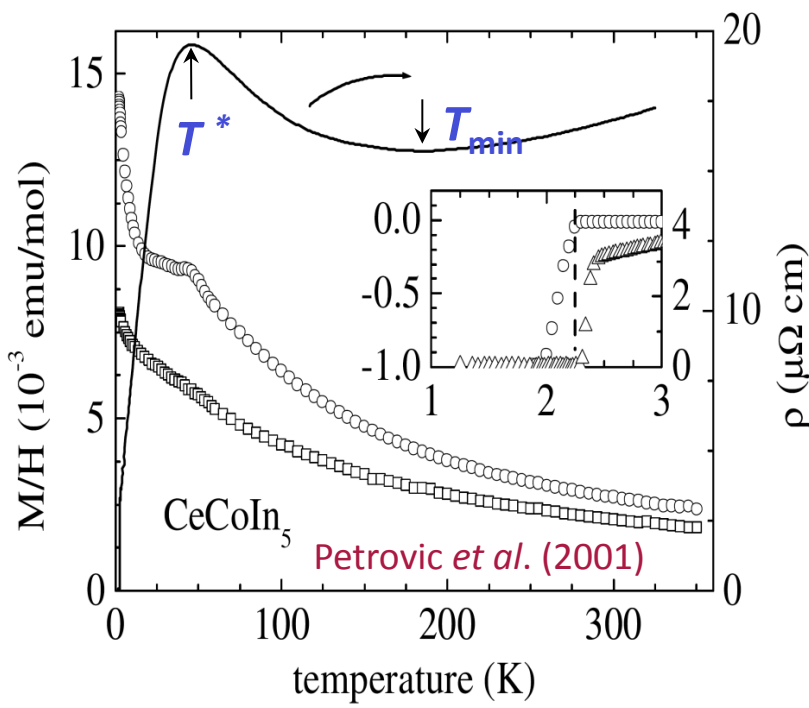
- Asymmetry is reproducible; conductance is always smaller when HF s are biased positively for the two SC 115s.

Relevance of Proposed Models

- Competing order (Hu & Seo, PRB 2006)
 - Does not explain STS data on UD-Bi2212, nor our CeIrIn₅ data.
- Non-Fermi liquid behavior (Shaginyan, Phys. Lett. A 2005)
 - Asymmetry is still seen in field-induced Fermi liquid regime.
- Large Seebeck effect in HF + thermal regime (Itskovich-Kulik-Shekhter, Sov. JLTP 1985): asymmetry persists in SC states.
- Energy-dependent QP scattering (Anders & Gloos, Physica B 1997)
 - Explains both reduced signal & asymmetry, but unclear origins.
- Strongly energy-dependent DOS (Nowack & Klug, LT Phys. 1992)

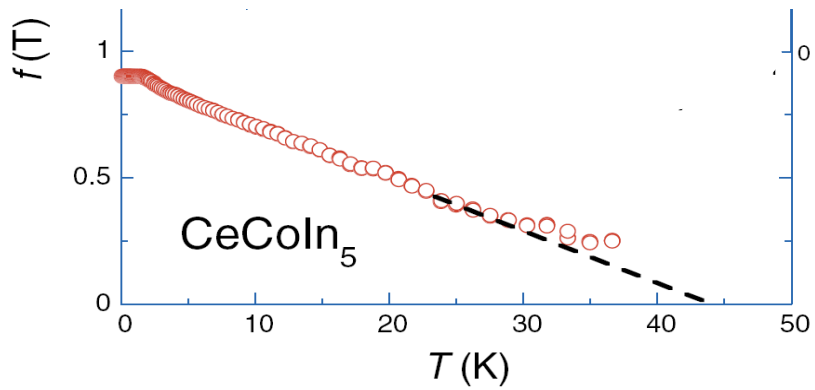


Two-fluid picture of heavy fermions



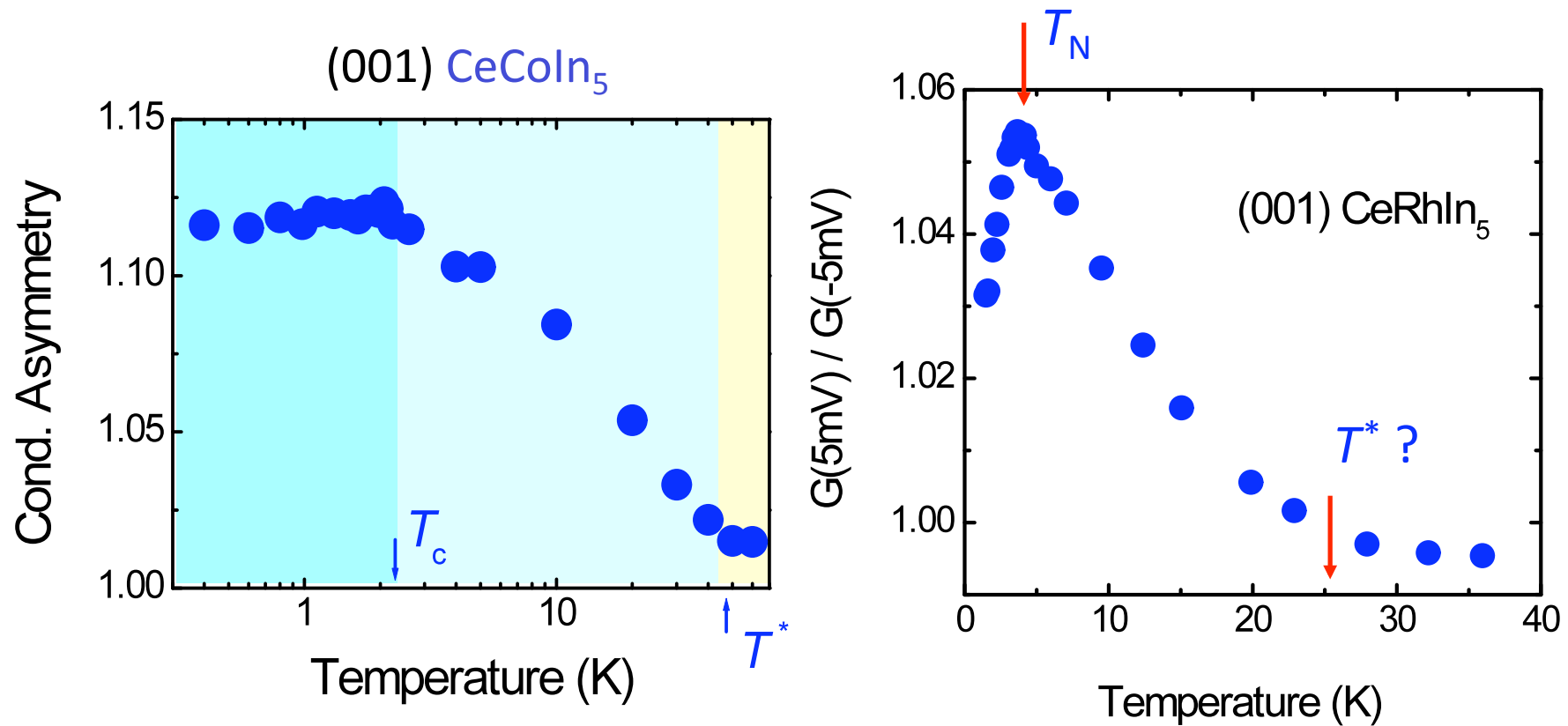
Shishido *et al.* (2002)

- Emerging heavy fermions in Kondo lattice systems below a coherence temperature, T^* (~ 45 K in CeCoIn₅).
- $f(T)$: relative weight of heavy-fermion liquid, increases with decreasing T and saturated below 2 K. Nakatsuji, Pines, Fisk, **PRL 92, 016401 (2004)**.



- This two-fluid picture appears valid in other heavy-fermion systems. Curro *et al.*, **PRB 70, 235117 (2004)**.
- “Heavy electrons superconduct but light electrons don’t.” Tanatar *et al.*, **PRL 95, 067002 (2005)**.

Conductance Asymmetry vs. Two-Fluid Behavior

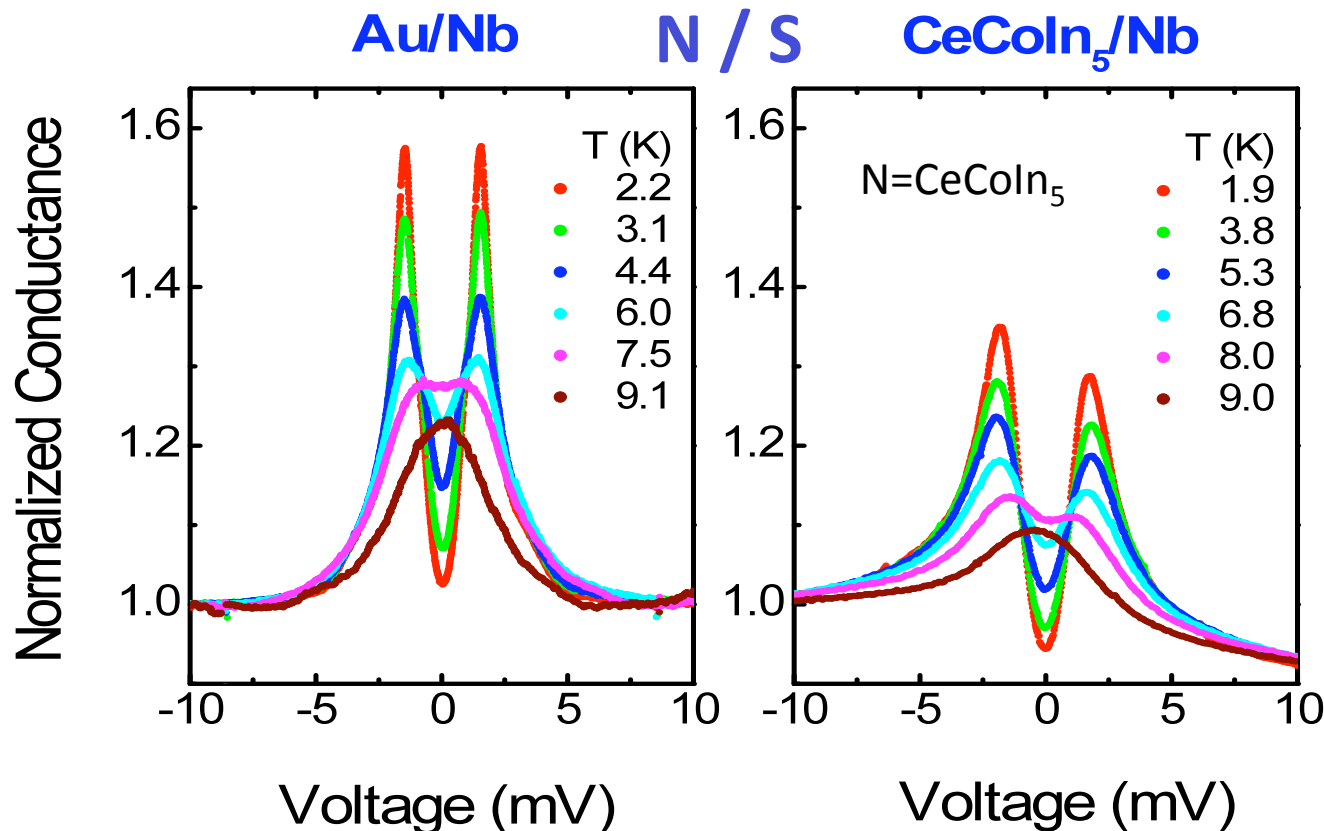


- Asymmetry follows HF spectral weight qualitatively.
- Saturation or decrease below SC or AFM transition.
- NdRhIn₅ (non-HF AFM) show no asymmetry.

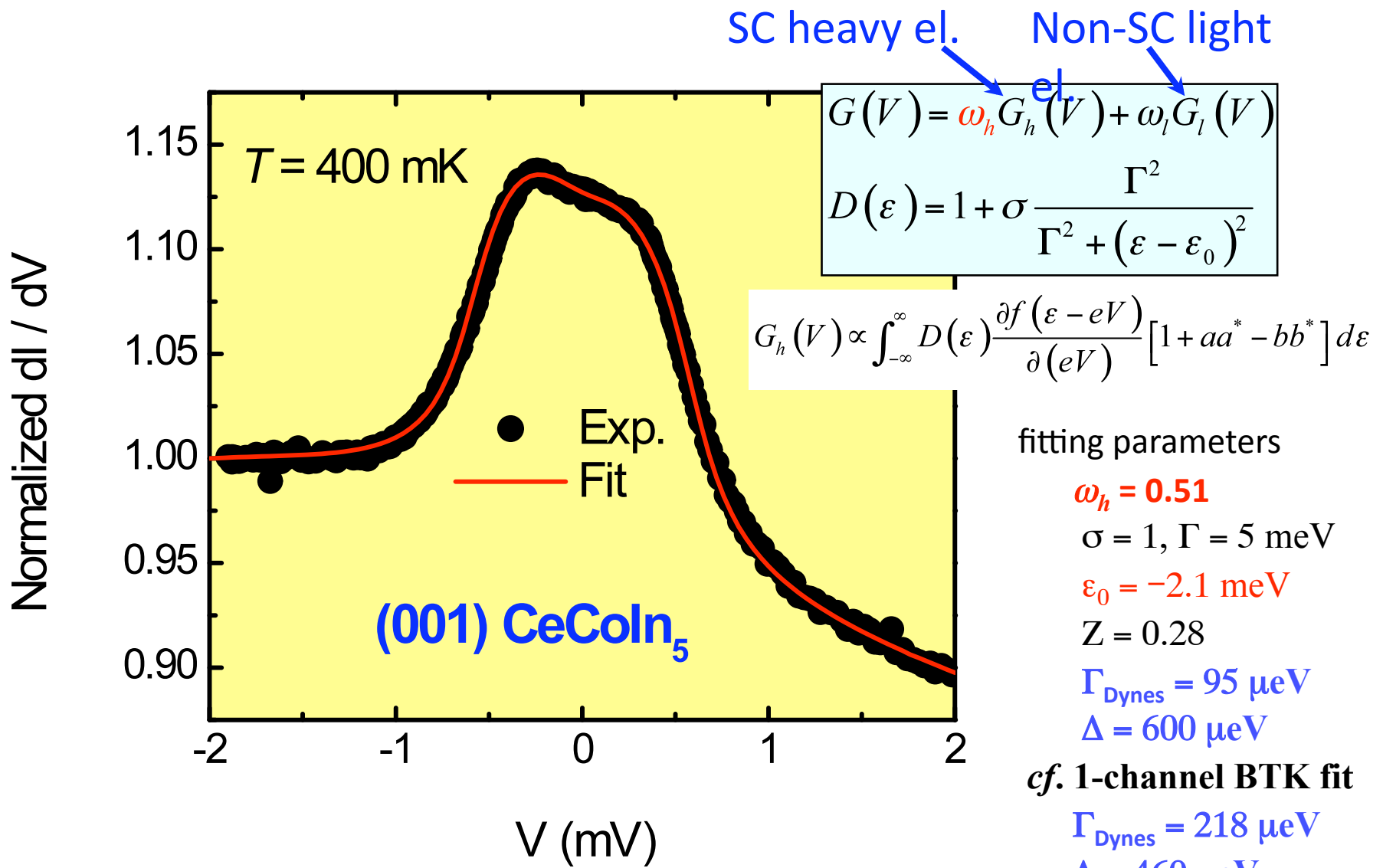
More support for 2-fluid model in CeColn₅

PCARTS for both N/S junctions of Au/Nb & CeColn₅/Nb are comparable, where there is no 2-fluid model for S Nb so all the Cooper pairs participate in the AR.

Recall for N/S Au/CeColn₅ is greatly reduced and we argue that
“one of the 2 fluids does not participate in the AR”



Two-channel Model Based on Lorentzian DOS



fitting parameters

$$\omega_h = 0.51$$

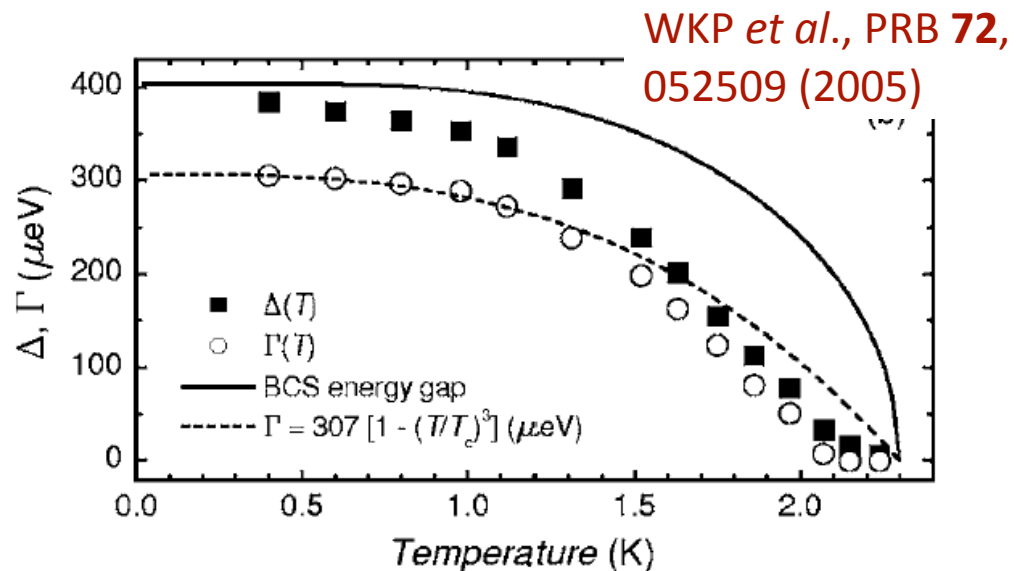
$$\Gamma_{\text{Dynes}} = 95 \mu\text{eV}$$

$$\Delta = 600 \mu\text{eV}$$

cf. 1-channel BTK fit

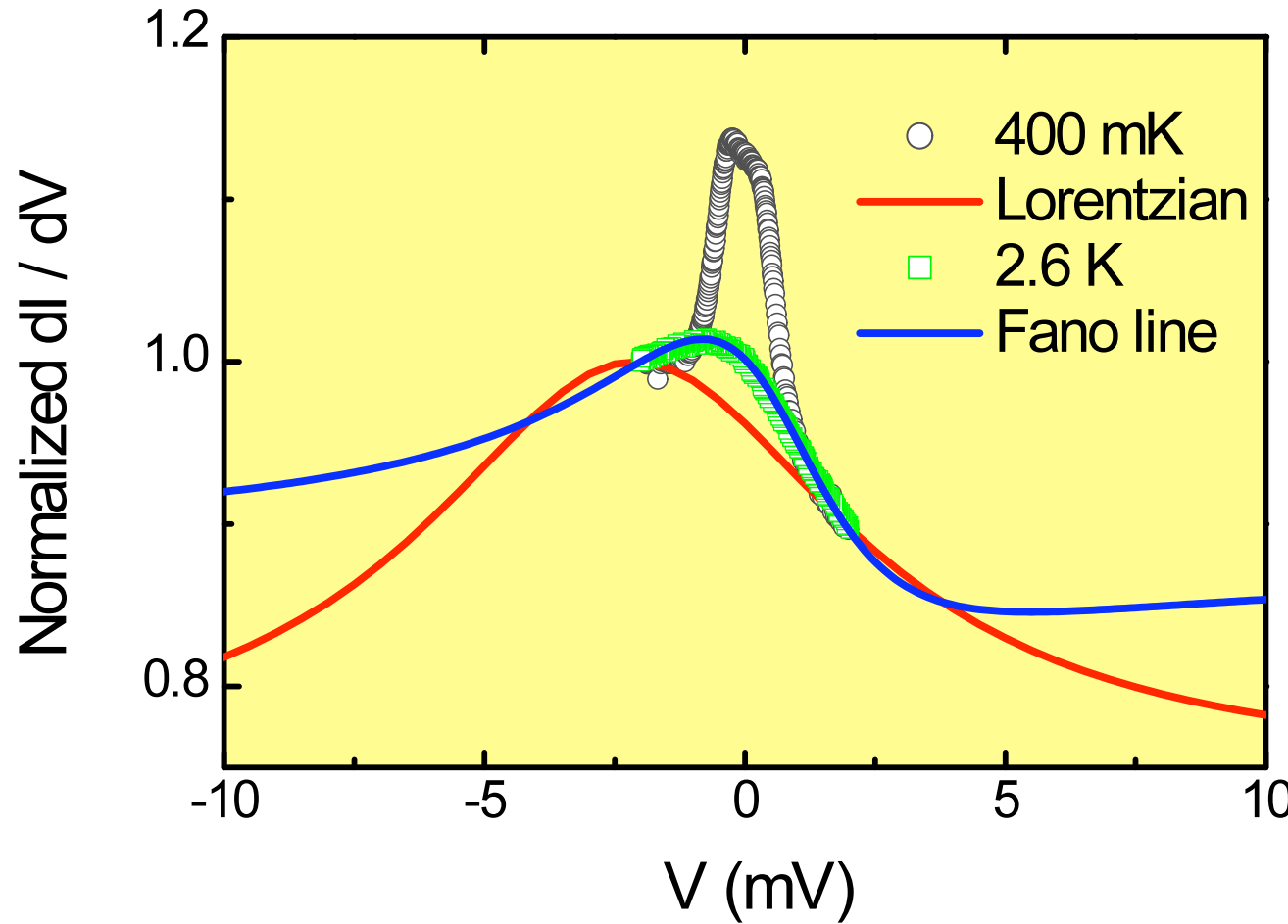
$$\Gamma_{\text{Dynes}} = 218 \mu\text{eV}$$

$$\Delta = 460 \mu\text{eV}$$



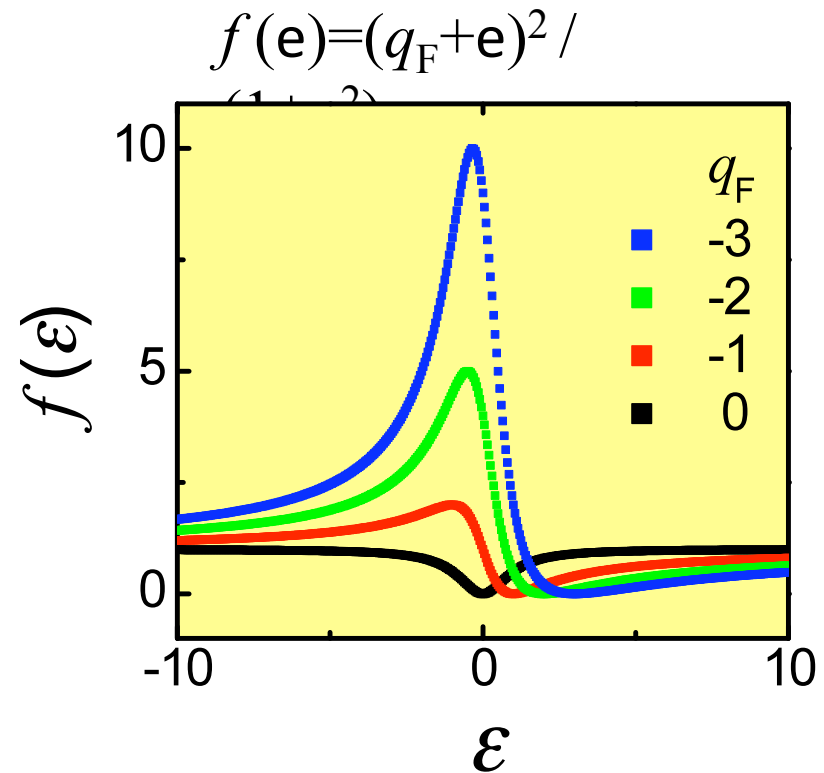
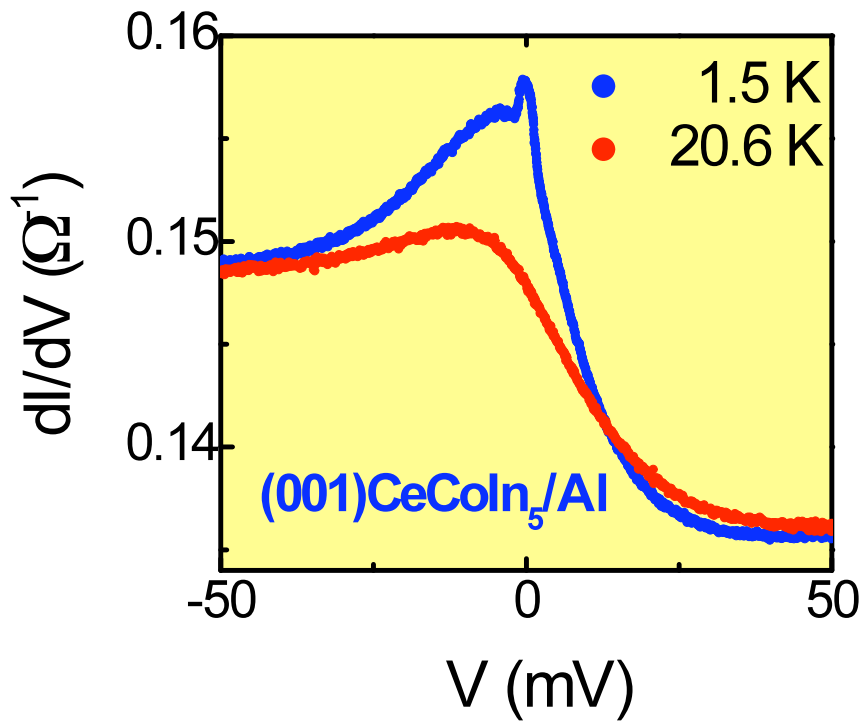
- Quality of the fit is sensitive to ω_h .
- Much smaller Γ_{Dynes} than that obtained from one-channel BTK fit → Fit does not suffer from unphysical temp. dependence of Γ_{Dynes} .
- Generality of two-fluid behavior (Curro et al., Yang & Pines) and reduced AR & cond. Asymmetry → Our model may be generally applicable to other HFS.
- BTK-like calculation based on two-fluid picture (Araujo & Sacramento, PRB 77, 134519 (2008)): claim both channels should be put implicitly into kernel (interference), but no account for asymmetry

High-Temperature Deviation



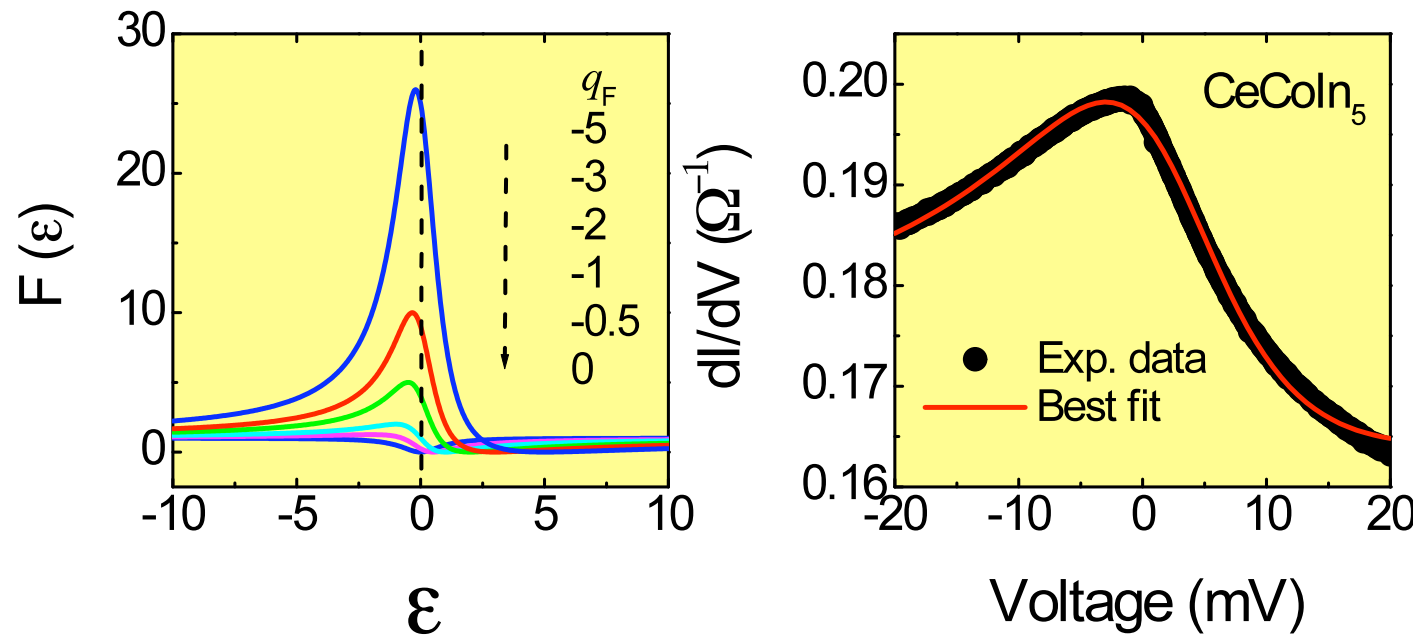
- Do not fit to a Lorentzian but to a Fano line-shape.

Fano Effect in Kondo Lattice?



- Conjecture: Fano interference effect between two conduction channels: heavy-electron band and conduction electron band.
- Fano factor can have negative value (interference), and peak position below Fermi level can mean the Kondo resonance above Fermi level.
- Underlying microscopic picture is being investigated, which should provide valuable insight into the Kondo lattice physics.

Conductance Model based on Fano Formula



$$F(\varepsilon) = (q_F + \varepsilon)^2 / (1 + \varepsilon^2), \quad \varepsilon \equiv (E - E_0) / (\Gamma/2), \quad dI/dV = C \cdot F(\varepsilon) + G_0$$

- $q_F = -2.14$, $E_0 = 2.23$ meV, $\Gamma/2 = 11.13$ meV, $C = 0.0061 \Omega^{-1}$, $G_0 = 0.164 \Omega^{-1}$
- negative q_F value - interference; positive E_0 - Kondo resonance above E_F ; large G_0 - large portion is not involved in interference.
- **Fano interference effect** between two conduction channels, into heavy-electron band and conduction electron band.

Fano Resonance

PHYSICAL REVIEW

VOLUME 124, NUMBER 6

DECEMBER 15, 1961

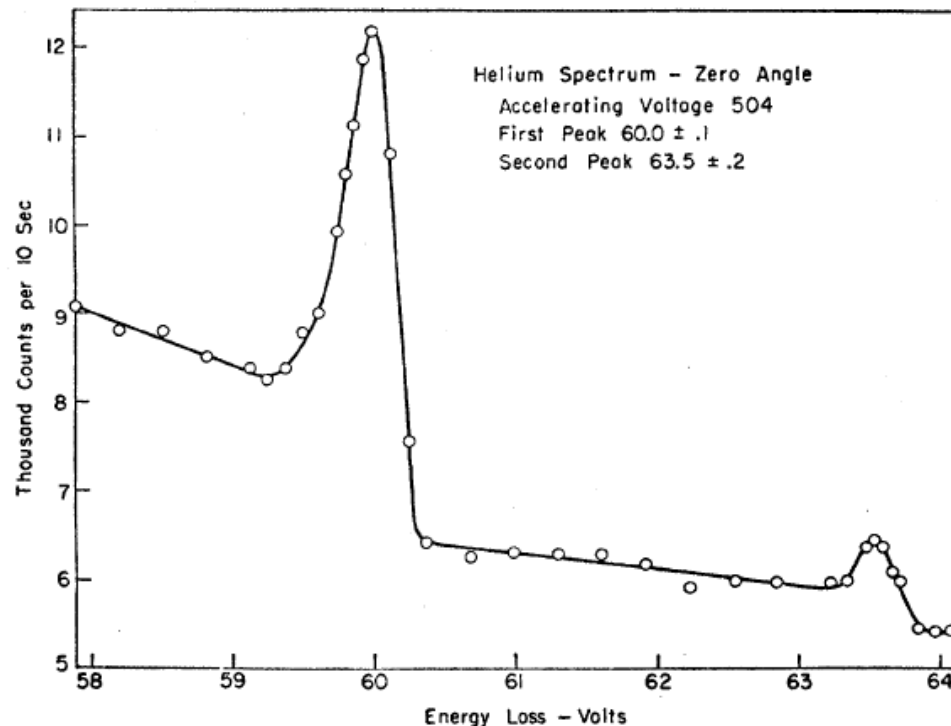
Effects of Configuration Interaction on Intensities and Phase Shifts*

U. FANO

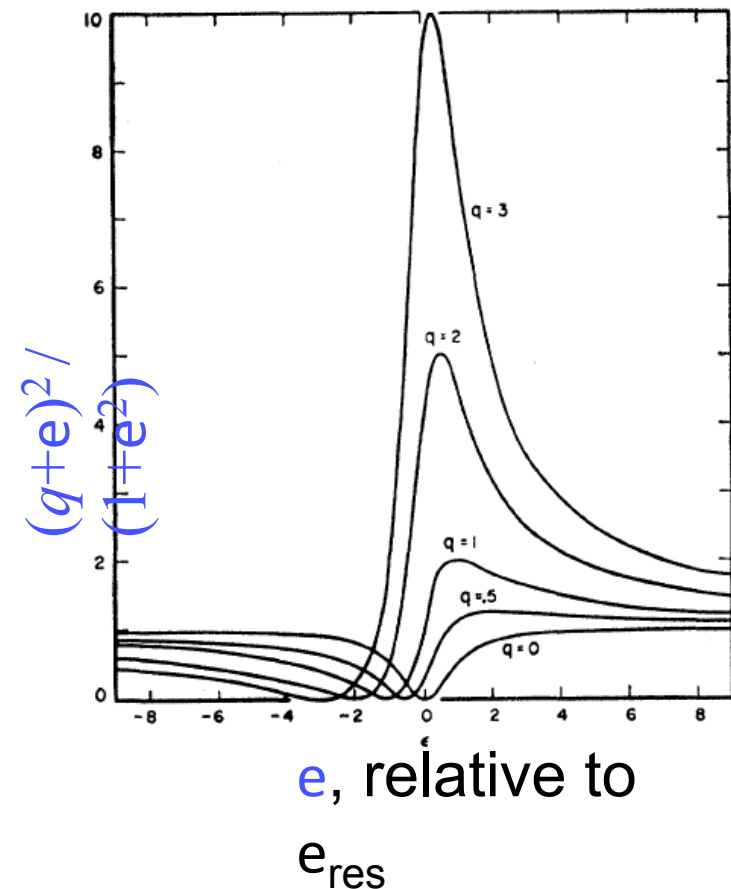
National Bureau of Standards, Washington, D. C.

(Received July 14, 1961)

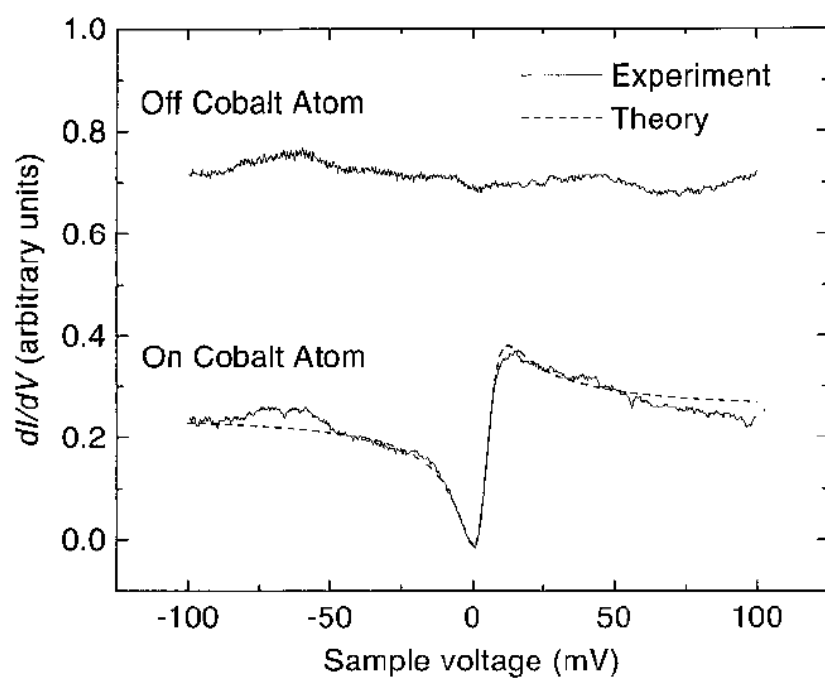
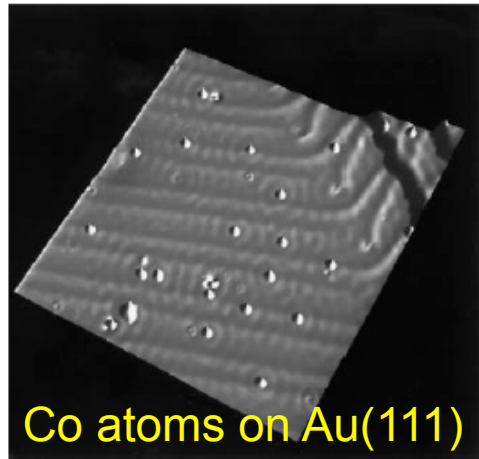
Electron-Helium inelastic scattering



Probability ratio for transition
to discrete and continuum



Fano / Kondo Resonance in Single Impurities



V. Madhavan et al., Science 280, 567 (1998)

$$\frac{dI}{dV}(V) = \frac{4e^2}{\hbar} \rho_{\text{tip}} \left[\pi \sum_k |\hat{M}_{tk}|^2 \delta(eV - \varepsilon_k) \right] \frac{(\varepsilon' + q)^2}{1 + \varepsilon'^2} + C$$

$$qe^{i\theta} = \frac{A}{B}$$
$$A(\varepsilon) = M_{at} + \sum_k M_{kt} V_{ak} P\left(\frac{1}{\varepsilon - \varepsilon_k}\right)$$

$$B(\varepsilon) = \pi \sum_k M_{kt} V_{ak} \delta(\varepsilon - \varepsilon_k).$$

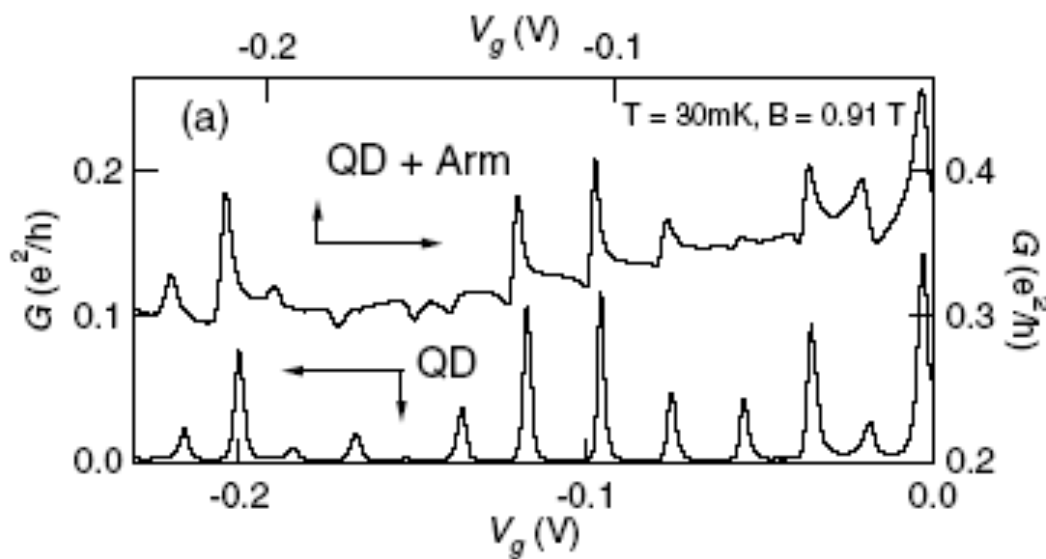
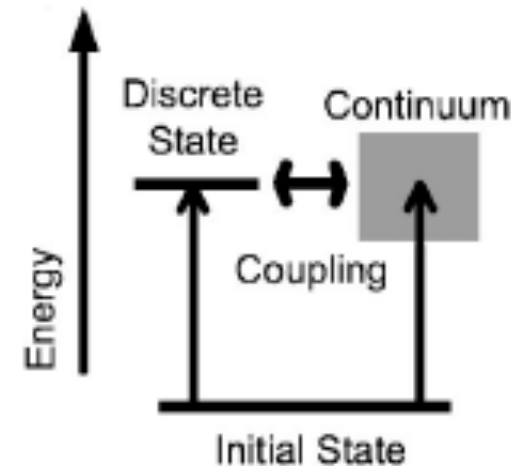
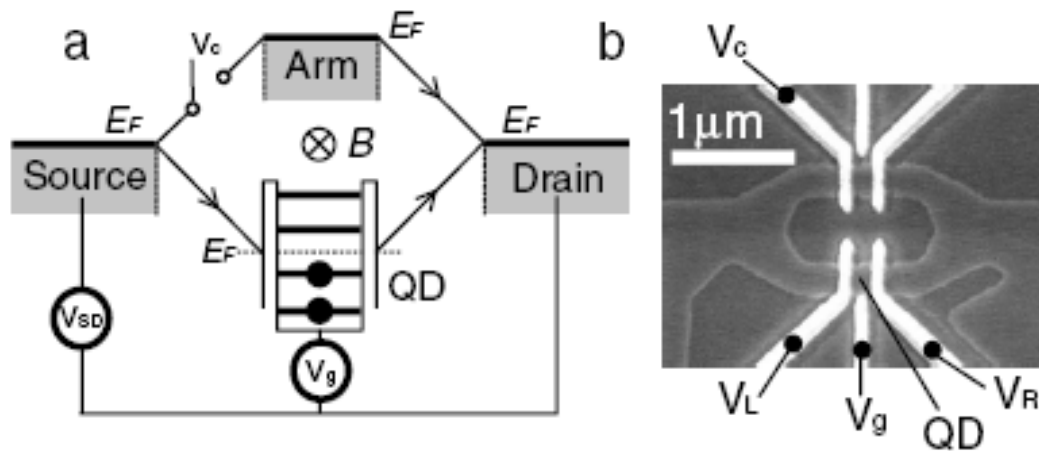
A: coupling to atomic orbital, direct or indirect via virtual transitions involving band electrons

B: coupling to conduction electron continuum

Other groups: Schneider, Eigler, Lieber, Kern, Zhao, Berndt, ...

Fano Resonance in Quantum Dots

K. Kobayashi et al., PRL 88, 256806 (2002)



“The Fano effect is essentially a single-impurity problem describing how a **localized** state embedded in the continuum acquires **itinerancy** over the system.”

Conclusions

□ Strength of the PCARS method

- First spectroscopic demonstration of $d_{x^2-y^2}$ symmetry in CeCoIn₅
- Density of states effects measured!
(energy-dependent DoS; peak)

□ Kondo Lattice Properties:

- Two-fluid model
- Energy-dependent DoS given by a Fano resonance possibly due to the interference of the f-electrons with the conduction electrons.